New Combined Heat Transfer Enhancement Techniques used in Laminar Flow through Non-Circular Ducts

[*]**Hrishiraj Ranjan**
e-mail: hrishi.ssec@gmail.com

[*]**Anand Kumar Bharti**
e-mail: anandkumar.kumar908@gmail.com

[*]**Madhu Sruthi Emani**
e-mail: **sruthi.emani@gmail.com**

[1]**Prof Josua Petrus Meyer**
e-mail: josua.meyer@up.ac.za

Department of Mechanical and Aeronautical Engineering
University of Pretoria, Private Bag X20
Hatfield 0028, South Africa

[*]**Sujoy Kumar Saha**
e-mail: **sjykmrsh@gmail.com**

[*]Mechanical Engineering Department
Indian Institute of Engineering Science and Technology, Shibpur
Howrah 711103, West Bengal, India

[1]Corresponding Author

Highlights

- Laminar flow through non-circular ducts with inserts is studied experimentally.
- Uniform wall heat flux boundary condition is imposed on the channel outer wall.
- Wide Prandtl number range is covered using viscous Servotherm medium oil.
- Heat transfer and pressure drop characteristics against Reynolds number are plotted.
- Correlations developed and performance evaluation is done and these are beneficial.

ABSTRACT

The problem of heat transfer enhancement using different combinations of transverse ribs, transverse corrugations and twisted-tape insert with oblique teeth, twisted tape with centre clearance and helical screw-tape insert in square and rectangular channel was investigated. The study also involved the thermohydraulic performance of inserts in non-circular channels in the laminar regime. Non-circular channels having aspect ratios of 1, 0.5 and 0.33 were considered. The techniques used for heat transfer augmentation in the present study were and the problem was (1) transverse ribs with twisted tape with oblique teeth, (2) integral transverse corrugation and centre-cleared twisted-tape insert, (3) transverse rib and helical screw-tape insert, (4) axial ribs and centre-cleared twisted-tape insert and (5) integral transverse rib and centre-cleared twisted-tape insert. These combined fin geometry are supposedly important from possible heat transfer enhancement point of view. In the channels, the combined influence of insert geometry such as rib pitch, rib height, twist ratio of twisted tape, twisted tape tooth horizontal length and twisted tape tooth angle was studied. The experiment was carried out using Servotherm oil as the working fluid, which had a wide range of Prandtl number (430–530). Uniform heat flux boundary condition was used. The methods used in the

experiment have been discussed in the text of the presentation. The important results of the experimental investigation showed that the thermohydraulic performance using a combination of inserts was better than that of bare ducts and that of the individual enhancement technique acting alone. Both the increase in pressure drop and heat transfer augmentation occurred due to the addition of inserts, but heat transfer enhancement dominated over the increase in pressure drop. Nusselt number and friction factor correlations have also been developed and are presented in this paper. The experimental program considered different fin arrangements with various parameters and therefore, it should be very helpful in designing heat exchangers of different shapes and sizes used for industrial purpose. It is concluded from the present investigation that 31–52 per cent increase in heat duty at constant pumping power and 25–36 per cent reduction in pumping power at constant heat duty are achievable. This is the novelty of the present work since no such study and the observations have been made earlier. These types of combined fin configurations have not been tried before. The findings are likely to have good impact in the industry.

Keywords: *Transverse rib, corrugation, centre-cleared twisted-tape insert , helical screw-tape insert, convection, swirl flow*

1. INTRODUCTION

In the present-day energy scenario, heat sources and renewable energy are the prime focus and the global scientific community is trying hard to optimize the use of existing sources of energy. Heat transfer enhancement devices are necessary for the energy-hungry modern days. Therefore, research on more efficient and effective heat transfer enhancement devices is very important. Heat transfer enhancement can be achieved by using active techniques and passive techniques. Active techniques are those in which external power sources are used. In passive techniques, no external power sources are required. The internal modification in tubes, channels or ducts enhances the rate of heat transfer. There is a good amount of literature on enhancing the thermal transport rate in both laminar flow and turbulent flow. These investigations have been carried out in circular, non-circular and other geometrical shaped internal flow cases, [1-4].

Passive heat transfer enhancement techniques are used in industrial heat exchangers and these have been investigated by many researchers. Saha [5] used a combination of transverse ribs and wire-coil inserts in rectangular and square ducts. He claimed that better heat transfer augmentation could be achieved using the above combination than by using bare ducts in the laminar flow regime and by using the individual enhancement technique acting alone. Pal and Saha [6] experimentally investigated heat transfer in the laminar regime with a circular tube having spiral ribs and twisted-tape insert and they found that the performance of a combination of inserts was much better than that of the individual enhancement technique acting

alone. They presented friction factor and Nusselt number correlations. Saha *et al.* [7] and Xie *et al.* [8] worked with circular tubes equipped with regularly spaced twisted-tape inserts and they concluded that the performance of regularly spaced twisted-tape inserts was much better than that of full-length twisted-tape inserts at high Reynolds number, larger twists and small tape-element spacings. They presented correlations for Nusselt number and friction factor. Modern twisted-tapes such as V-cut twisted tape and perforated twisted tapes were used by Thiangpong *et al.* [9]; serrated twisted tape was investigated by Eiamsa-Ard and Promvonge [10]; short-length twisted tape in round tubes was investigated by Eiamsa-Ard and Seemawute [11]; twisted tape with alternate axis was examined by Krishna *et al.* [12]. Bhuiya *et al.* [13] worked with double-counter twisted tape to evaluate heat transfer and fluid friction characteristics in heat exchanger tubes and they found that the increase was up to 240 per cent and 286 per cent for heat transfer and friction factor, respectively in comparison with that of plain tubes. Ray and Date [14] numerically analyzed friction factor and heat transfer characteristics of laminar flow and turbulent flow through a square duct with twisted-tape inserts. Earlier works on the predictive methods, data and correlation on laminar flow regime with twisted tapes were due to Hong and Bergles [15], Date [16], Date and Gaitonde [17] and Saha and Dutta [18]. They gave correlations and prediction methods for calculating heat transfer and friction factor. Han [19] investigated rectangular channels with rib turbulators and Shivkumar and Raja Rao [20] investigated twisted tapes in rough tubes. Saha *et al.* [21] worked with axial corrugation roughness and twisted-tapes with and without oblique teeth in a non-circular duct. They found that the

heat transfer rate in the case of axial corrugation, combined with twisted-tape with oblique teeth, was higher than the heat transfer rate in case of the combined case without oblique teeth. Saha and Saha [22] experimentally investigated the heat transfer rate in laminar flow in a circular tube using a combination of integral helical rib roughness and helical screw-tape. They found that the performance of combined inserts was significantly better than that of the passive enhancement techniques acting alone in a circular duct. They established correlations which can be used for industrial applications. Saha and Dayanidhi [23] investigated the performance of centre-cleared twisted-tape and integral helical corrugation used together. They achieved a 150 per cent to 200 per cent increase in Nusselt number by using this combination. Saha *et al.* [24] used wire-coil inserts in combination with centre-cleared twisted tape to study the heat transfer enhancement in a circular tube in laminar flow regime. They claimed that the friction factor was increased by 15 per cent to 25 per cent and Nusselt number was increased by 45 per cent to 65 per cent when using inserts. Patil [25] used twisted-tape insert with varying tape width in laminar flow for augmentation of heat transfer and the working fluid was pseudo plastic power-law fluid. The uniform wall temperature boundary condition was imposed and Patil [25] obtained poor heat transfer enhancement with the reduced width tape. Wongcharee and Eiamsa-Ard [26] and Eiamsa-Ard *et al.* [27] investigated the thermohydraulic performance of clockwise and counterclockwise, alternate-axis twisted-tape insert. They concluded that the friction factor was higher for the twisted-tape insert with alternate axis than that for the plain tube and it further increased with a decrease in twist ratio; i.e. tighter twists. They also

concluded that the friction factor for the twisted-tape insert with alternate axis was increased by 50 per cent, 49 per cent and 33 per cent for the twisted tape having a twist ratio of y = 3.0, 4.0 and 5.0, respectively. They achieved an enhancement in heat transfer which was higher than that for a plain twisted tape having the same twist ratio. Webb and Kim [28] discussed all the heat transfer enhancement techniques and developed correlations for different fin configurations. All these investigations clearly indicate that inserts and ribs enhance the heat transfer rate at the cost of low pressure drop increase. [29-33] are most recent literature in the area of nanofluids.

The objective of this paper is to report the results of an experimental investigation on the hydrothermal behavior, performance analysis and correlations for laminar flow through channels having compound inserts for which there had been no previous investigations. The experimental program used various combinations of fin geometries: (1) transverse ribs with twisted-tape insert with oblique teeth, (2) integral transverse corrugation and centre-cleared twisted-tape insert, (3) transverse rib and helical screw-tape insert, (4) axial ribs and centre-cleared twisted-tape insert and (5) integral transverse rib and centre-cleared twisted-tape insert. This study is unique because no such research work, either experimental or theoretical has been reported so far. It is concluded from the present investigation that 31-52 per cent increase in heat duty at constant pumping power and 25-36 per cent reduction in pumping power at constant heat duty are achievable. This is the novelty of and the innovation in the present work since no such study and the observations have been made earlier. These

types of combined fin configurations have not been tried before. The findings are likely to have good impact in the industry.

2. EXPERIMENTAL SET-UP, WORKING PROCEDURE AND DATA ANALYSIS

The experiments were conducted with proper care and in normal laboratory atmospheric conditions. A full schematic diagram of the experimental rig is shown in Figure 1 with detailed positioning of instruments. In the pressure drop experiment, an acrylic duct of 2 m in length was used. The cross-section and aspect ratios were 13 mm × 13 mm for square duct (aspect ratio = 1), 13 mm × 26 mm (aspect ratio = 0.5) and 13 mm × 39 mm (aspect ratio = 0.33) for rectangular ducts, respectively. The heat transfer testing was done in stainless steel ducts having the same dimensions as those of the acrylic ducts for pressure drop tests. The heat transfer test section was electrically heated by a nichrome heater wire for achieving uniform wall heat flux boundary condition. In the case of heating, there was no direct physical contact between the nichrome heater and the testing section. The test section wall boundary had high thermal conductivity and it was thin enough to provide uniform heat flux. Porcelain bead insulation was applied to the nichrome heater and fiber glass tape insulation was applied on the duct wall. The test section was insulated with asbestos rope and glass-wool. The heater wire and whole test section were covered with a jute bag.

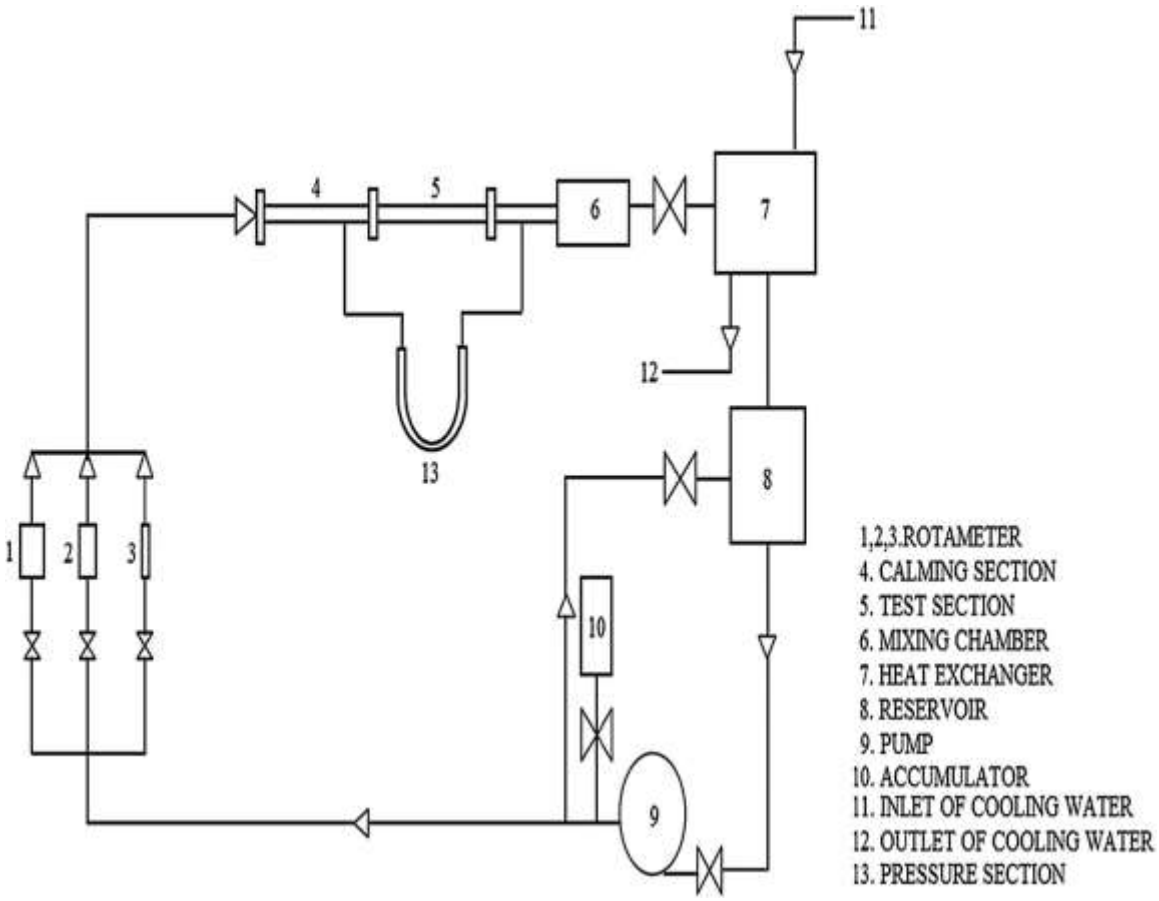

Fig. 1. Experimental rig.

The experimental test rig had a working fluid circulating loop, a cooling water circulating loop, rotameters, autotransformers with digital voltmeter and ammeter, thermocouples with digital multimeter and selector switch box and U-tube mercury manometer. The rotameters having a measurement range of 0.07 to 0.7, 0.0115 to 0.115 and 0.00175 to 0.0175 kg/sec, respectively were used for measuring and regulating the oil mass flow rate. The calming section ensured that the flow was hydrodynamically fully developed before it entered the heated test section.

The transverse rib, axial rib and integral transverse rib corrugations are presented in Figure 2, Figure 3 and Figure 4, respectively. The square-shaped ribs were

made of brass. The twisted-tape insert with oblique teeth, centre-cleared twisted-tape insert and helical screw-tape insert are shown in Figure5, Figure 6 and Figure 7, respectively.

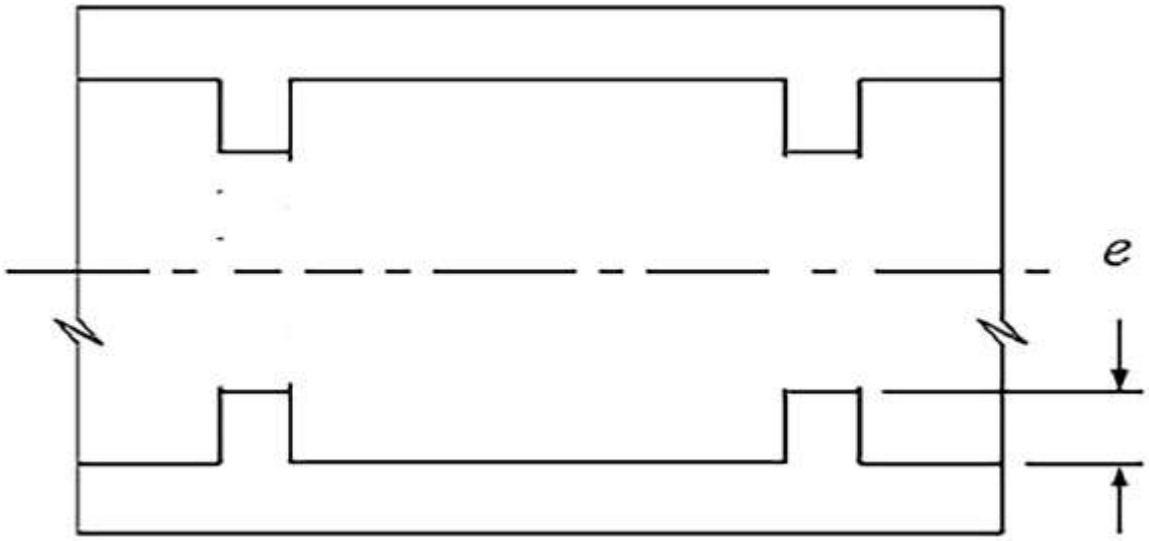

Fig. 2. Transverse rib.

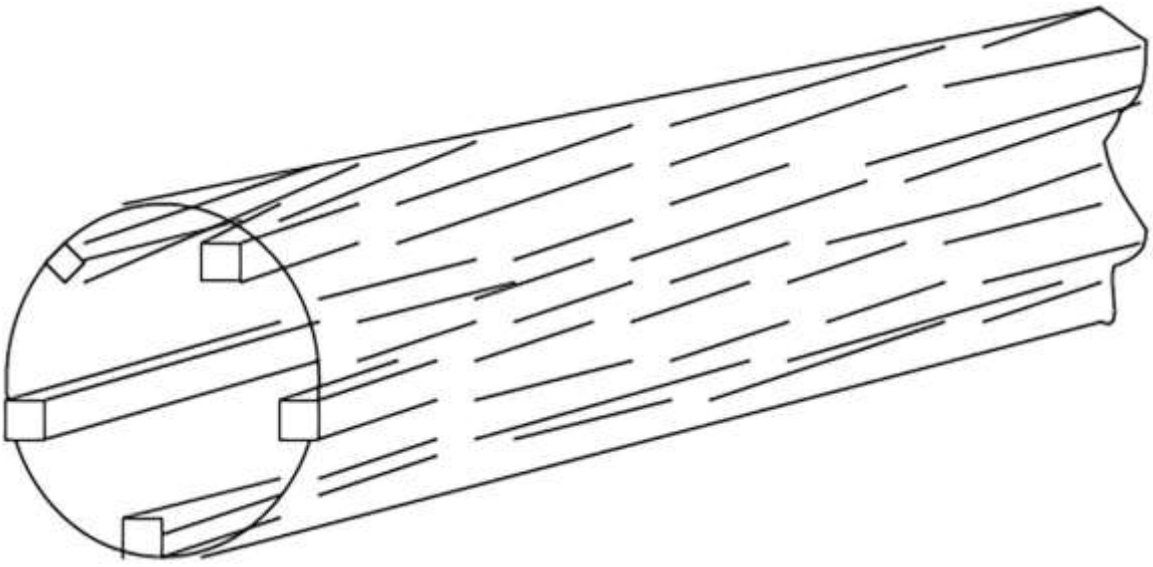

Fig. 3. Axial rib.

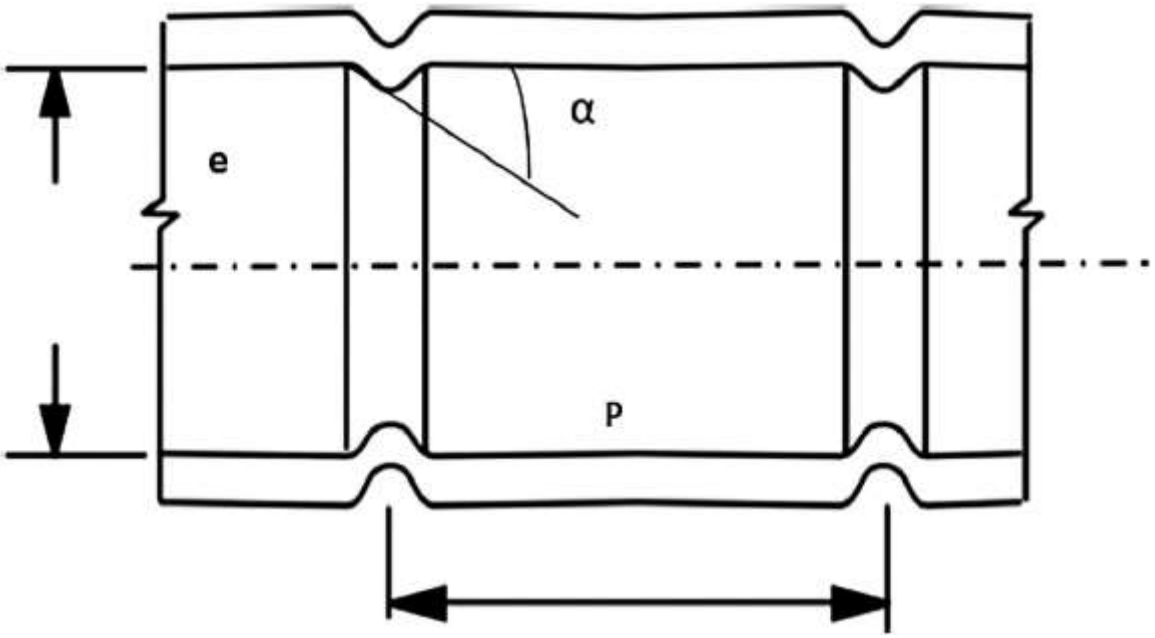

Fig. 4. Transverse rib corrugation.

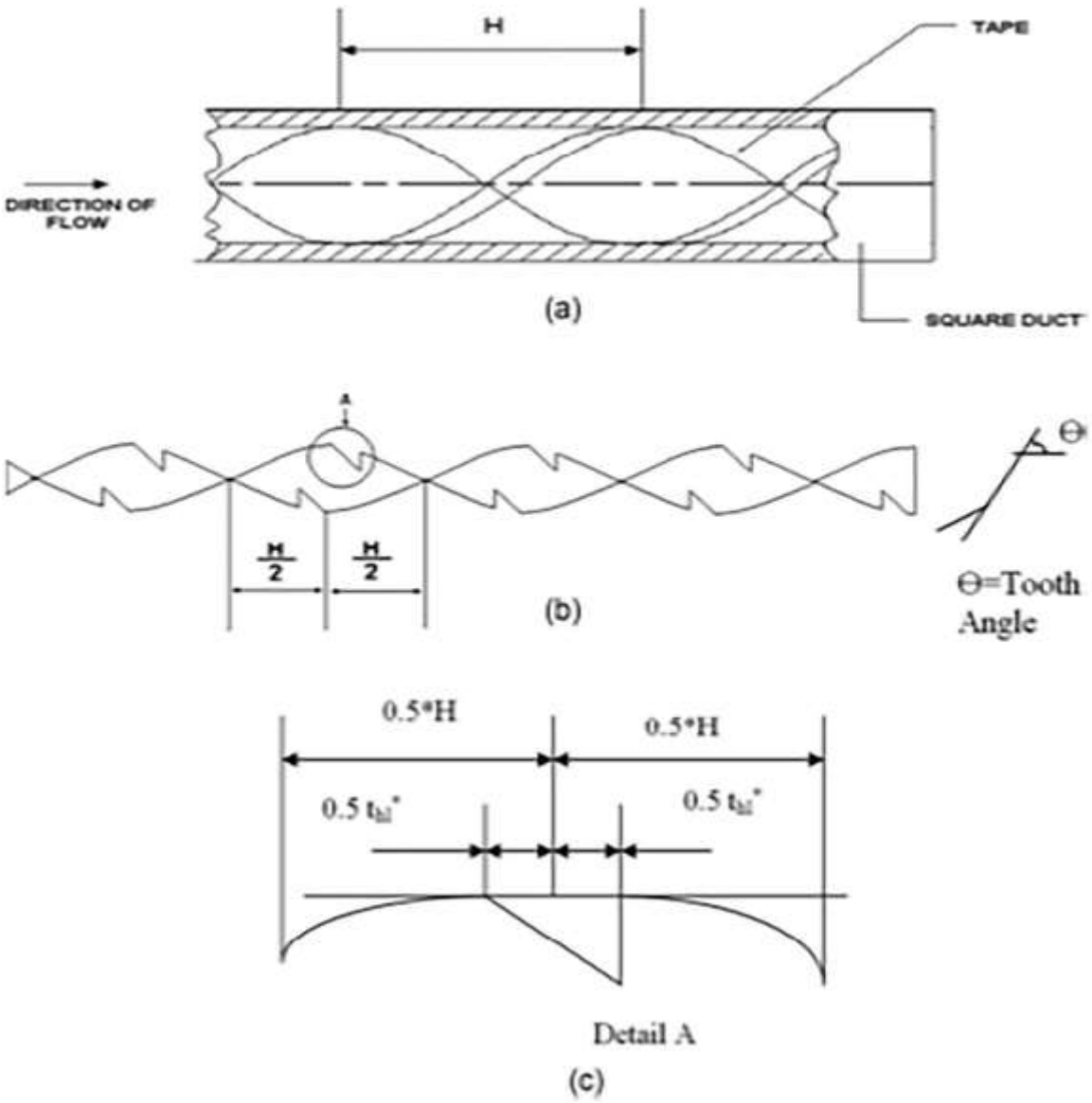

Fig. 5. Twisted tape.

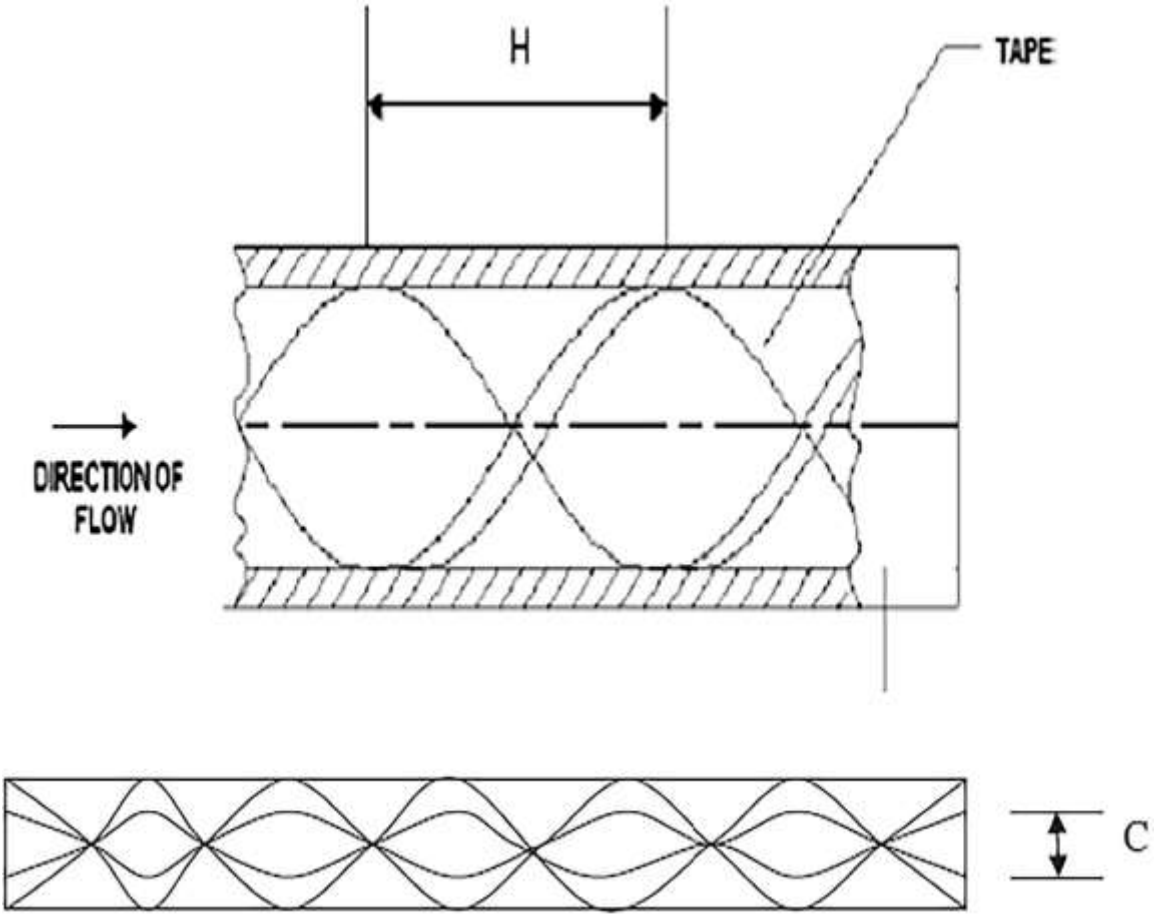

Fig. 6. Twisted-tape insert (with centre clearance).

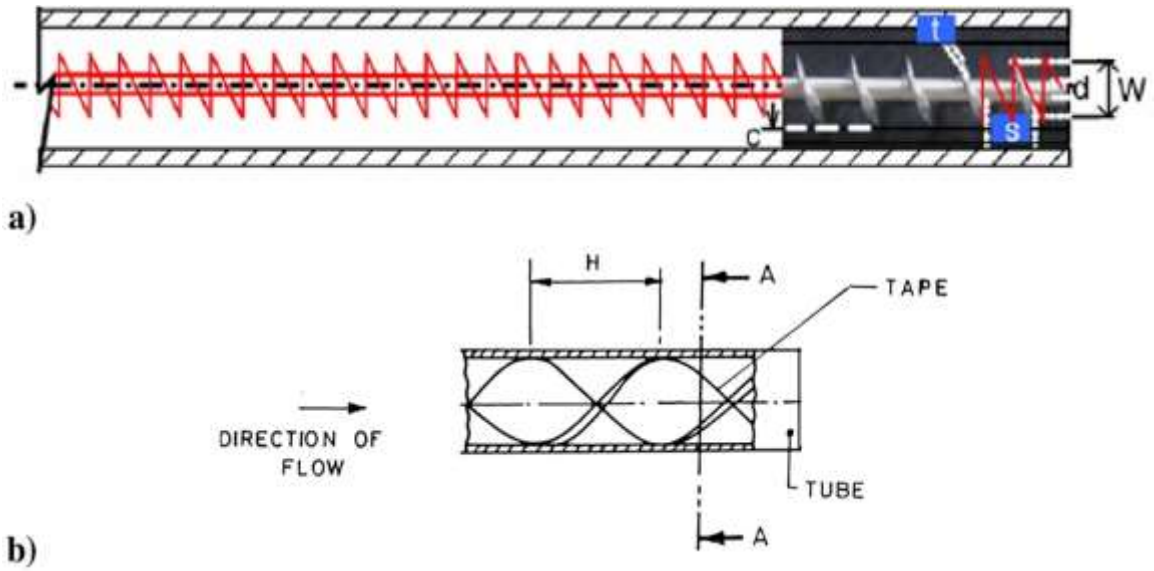

Fig. 7. Layout of a duct with full-length turbulator inserts.

The working fluid used in the experiment was Servotherm medium oil. It is a product of Indian Oil Corporation having a wide Prandtl number range of 430 to 530. Oil mass flow rate was measured by rotameters and the isothermal pressure drops were measured by a vertical mercury manometer. The actual heat received by the oil was its enthalpy rise. The working fluid was circulated through a pump and an accumulator was used to reduce the pressure fluctuations and oil hammering. The measurement of outer-wall temperature of the test section was done by copper-constantan thermocouples and a digital multimeter. Thermocouples were fitted at seven axial positions and each axial position was equipped with four thermocouples, which were installed by brazing. The axial locations of thermocouples were 5 cm, 50 cm, 100 cm, 125 cm, 150 cm, 175 cm, 195 cm along the downstream direction from the test section inlet. The thermocouples were 90° apart from each other. Oil bulk mean temperatures at inlet as well as outlet were measured by copper-constantan thermocouples. A mixing chamber was used for achieving uniform temperature of working fluid at the exit. In the mixing chamber, oil moved in a serpentine path giving uniform temperature. The duct wall temperature increased linearly in the downstream fully developed region. The test section heat input was calculated by measuring the resistance of heater wire and voltage across the heater wires. The uncertainties in the Reynolds number, Prandtl number, friction factor and Nusselt number were ± 4.3 per cent, ± 5.87 per cent, ± 6.33 per cent and ± 7.45 per cent, respectively and the uncertainties were determined by the method suggested by Kline and McClintock [34].

The experimental parameters for transverse rib and twisted tape with oblique teeth were as follows: twist ratio y = 2.5, twisted-tape tooth horizontal length t_{hl}= 0.1053 and 0.05263, twisted-tape insert tooth angle θ = 30^o and 60^o, rib height (e/D_h) = 0.07894 and 0.10526, rib pitch (P/e) = 20 and 10. Similarly, the parameters for axial rib with centre-cleared twisted-tape inserts and integral rib roughness and centre-cleared twisted-tape insert were the same and these were as follows: twist ratio y = 2.5, centre-clearance c = 0,0.2,0.4 and 0.6, rib height (e/D_h) = 0.07692 and 0.1026, rib pitch (P/e) = 5.6481 and 2.0437. Similarly, for transverse rib and helical screw-tape inserts, the parameters were as follows: screw-tape insert length = 2 m long, W = 8 mm (fixed), d = 0, 1.5 mm, 2 mm and 2.5 mm, c = 11 mm, 8.5 mm, 16.0 mm, screw-tape parameter p = ∞, 2.72, 2.04, 1.63 for AR = 1, p = ∞, 3.68, 2.76, 2.21 for AR = 0.5 and p = ∞, 6.16, 4.62, 3.62, rib height (e/D_h) = 0.07692 and 0.1026, rib pitch (P/e) = 5.6481 and 2.0437. The parameters for integral transverse corrugations and centre-cleared twisted-tape inserts were as follows: twist ratio y = 2.5, centre clearance c = 0,0.2, 0.4 and 0.6, corrugation angles θ = 30^o and 60^o, corrugation pitch (P/e) = 5.6481 and 2.0437.

The operating procedure for the experiment was as follows:

Initially, the set-up ran for an hour or more at the constant mass flow rate and uniform heat flux input so that the system attained steady state. Whether the system achieved steady state or not, could be verified by taking readings after a certain time interval, if the two readings taken at successive time intervals were the same, steady state was reached. Once steady state was reached, the digital multimeter was used for recording the outer-wall surface temperature, the fluid inlet and outlet temperatures.

The multimeter displayed the readings in millivolt and the equivalence value of the temperature could be obtained from conversion factor 40 μV = 1°C. After getting the inlet and outlet temperatures, the fluid local temperature was obtained at seven places by linear interpolation. This approach is supported by the fact that fluid bulk mean temperature increases linearly under uniform heat flux condition. The inlet and exit temperatures of the oil were measured by the thermocouple placed at the calming section just before the fluid entry and another thermocouple embedded at the exit of the oil mixing chamber to get the bulk mean temperature of the oil. The temperature drop across the tube wall thickness was determined by one-dimensional radial heat conduction equation. Additional information in this section can be obtained from [6].

3. Results and Discussion

The main objective of the present study was to see the effects of inserting oblique teeth twisted tape along with transverse ribs in non-circular channels. The relative effect of geometrical parameters such as aspect ratio, tooth angle, twisted tape tooth horizontal length, rib pitch and rib heights on thermal and hydraulic characteristics (Nusselt number and friction factor) was examined. Figure8 and Figure9 present the validation of the experimental data by using well documented correlations for friction factor and Nusselt number, respectively. Experimental data were obtained for a plain square duct and a plain circular tube. The deviation for most of the data is within $\pm$ 10 percent, thus warranting the validity of the experimental set up. Figure 10 shows the effect of twisted tape tooth horizontal length and tooth angle on friction factor for transverse rib and twisted tape with oblique teeth inserted into a channel

with aspect ratio (AR) = 1.0. It was found that the friction factor was higher for t_{hl}= 0.1053 and θ = 60°. The similar trend was observed for channels with AR = 0.5 and 0.33. The friction factor depended on channel cross-sectional geometry and it increased with a decrease in aspect ratio because of the flattening of the velocity profile. Figure 11 shows the Nusselt number vs Reynolds number relation for twisted-tape insert with oblique tooth combined with transverse ribs in a non-circular channel with AR = 1. The Nusselt number followed the same trend as that of the friction factor, because the Reynolds analogy prevailed. The values of twist ratio, rib height and rib pitch were kept constant so that the influence of tooth angle, tooth horizontal length and aspect ratio could be examined. The highest Nusselt number was found for aspect ratio AR = 0.33 at the tooth angle θ = 60° and t_{hl} = 0.1053. Figure 12 presents the friction factor for aspect ratios AR = 1.00, 0.5 and 0.33 at fixed geometrical parameters of the inserts. The highest friction factor and Nusselt number were obtained for aspect ratio 0.33. The effect of rib pitch and rib height on friction factor are shown in Figure 13 and Figure 14. A similar trend was observed for Nusselt number. A second set of experiments was carried out using integral transverse corrugation with centre-cleared twisted-tape inserts. The effect of centre clearance “c” on friction factor and Nusselt number is presented in Figure 15 and Figure 16, respectively. The centre clearance influenced the friction factor and the friction factor reduced with an increase in centre clearance because of less skin friction drag. The effect of corrugation angle on friction factor is presented in Figure 17, a larger corrugation angle resulted in a higher friction factor. Similarly, the Nusselt number was found to be the highest for the largest corrugation angle.

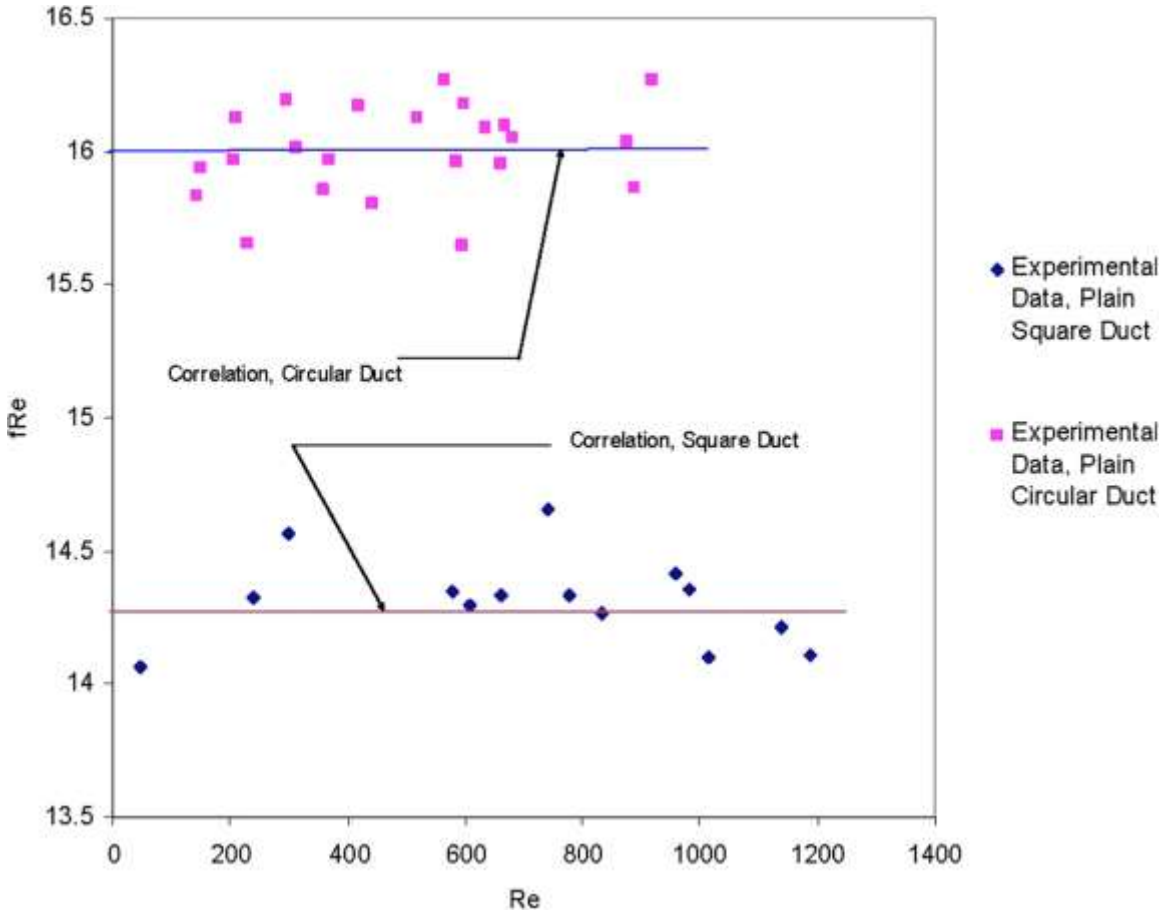

Fig. 8. Experimental set-up validation for friction factor.

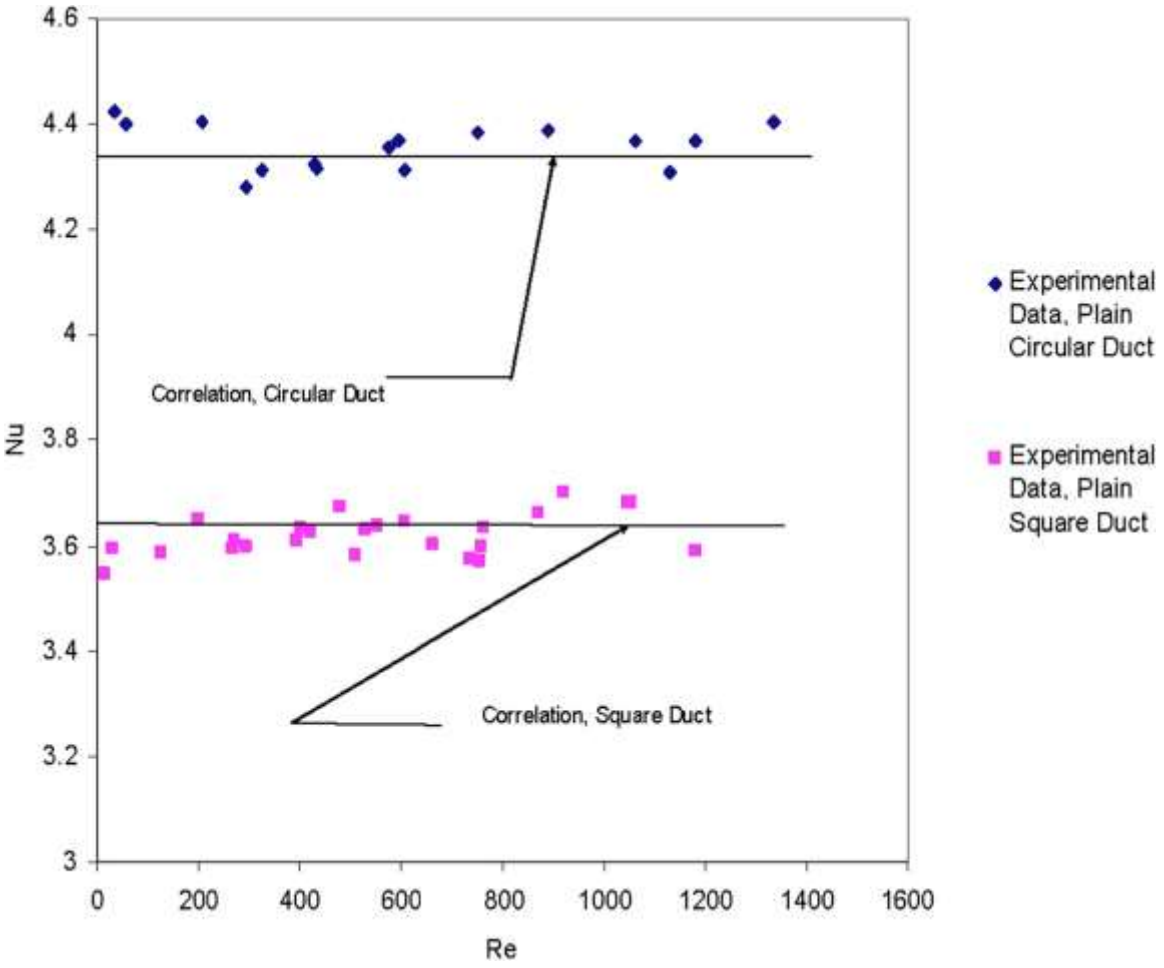

Fig. 9. Experimental set-up validation for Nusselt number.

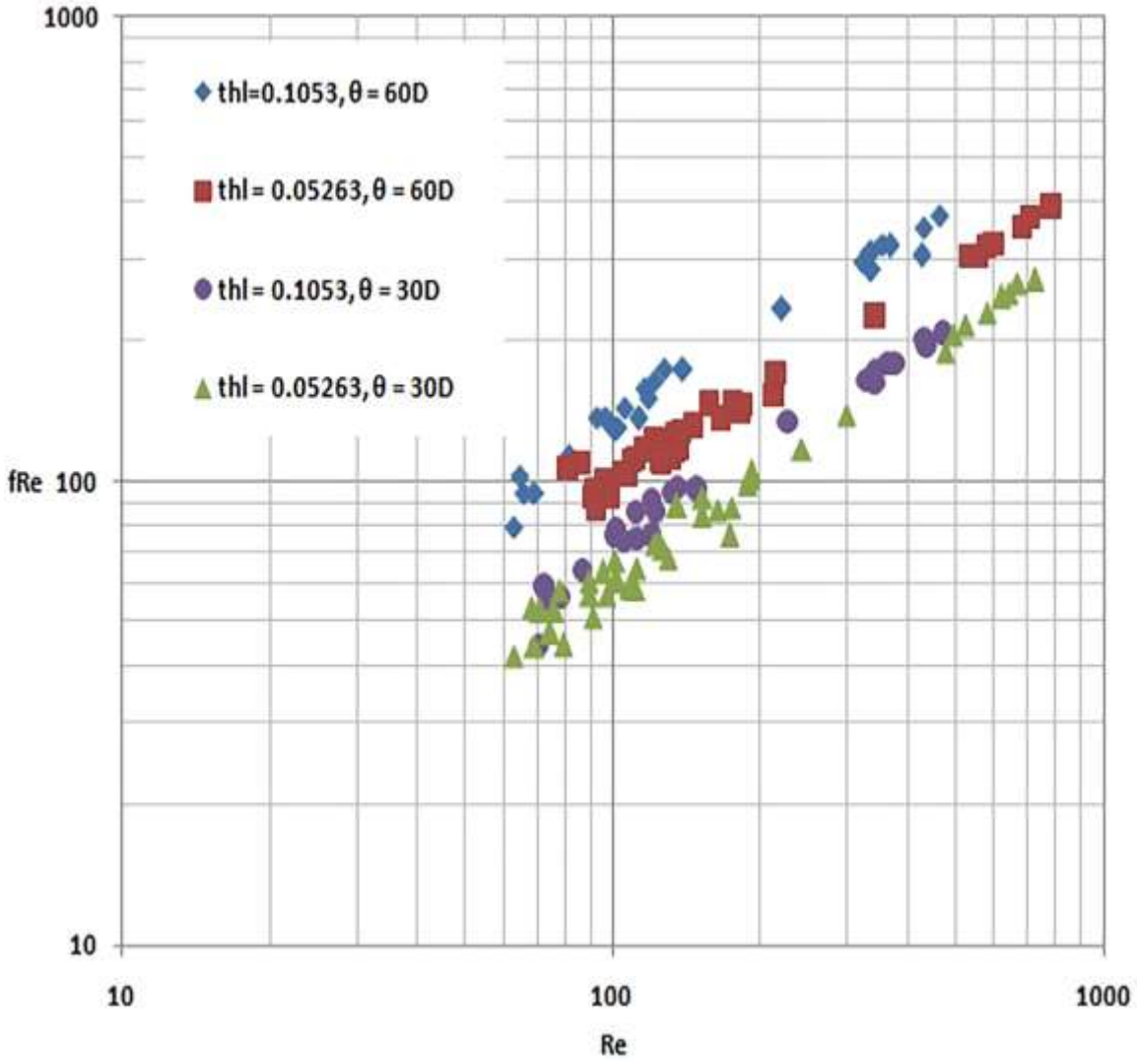

Fig. 10. Twisted-tape tooth length and angle effect, twist ratio 2.5, rib pitch 20, rib height 0.07894, aspect ratio 1.0.

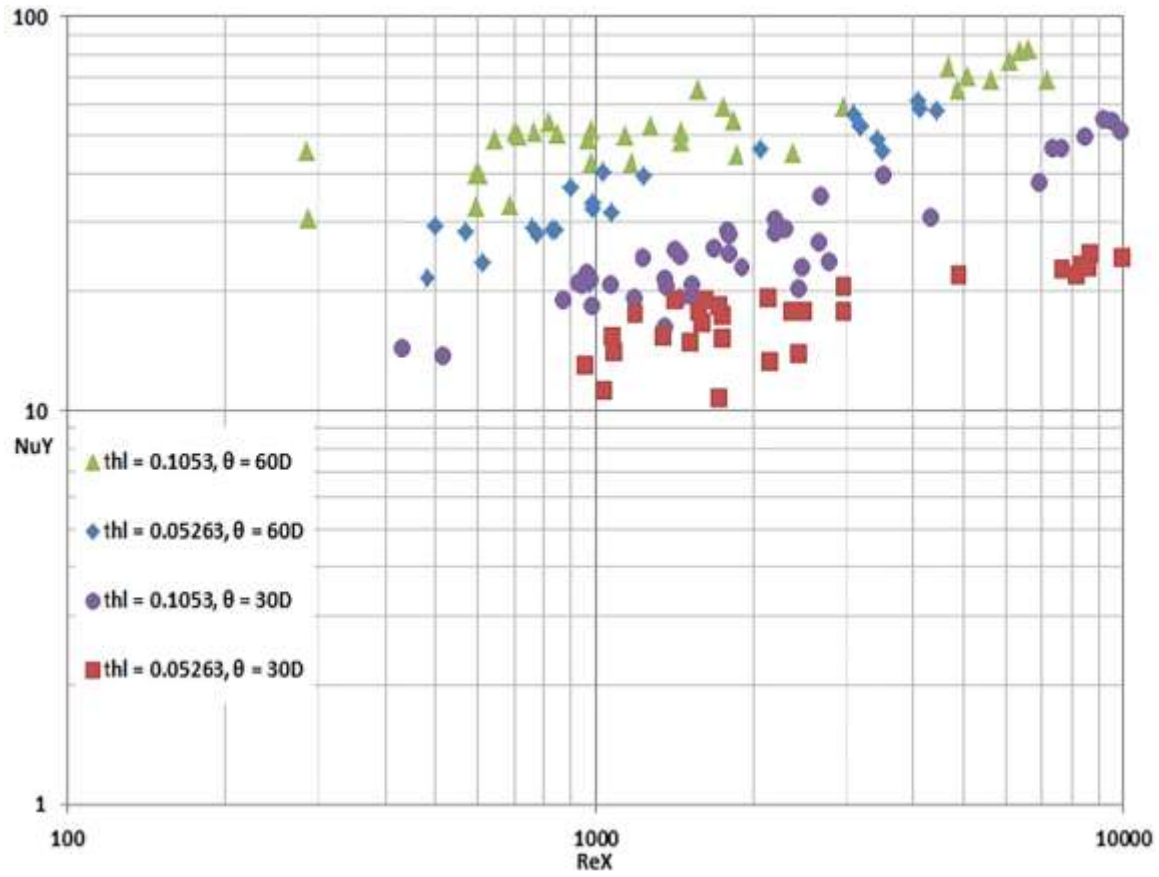

Fig. 11. Twisted-tape tooth length and angle effect, twist ratio 2.5, rib pitch 20, rib height 0.07894, aspect ratio 1.0.

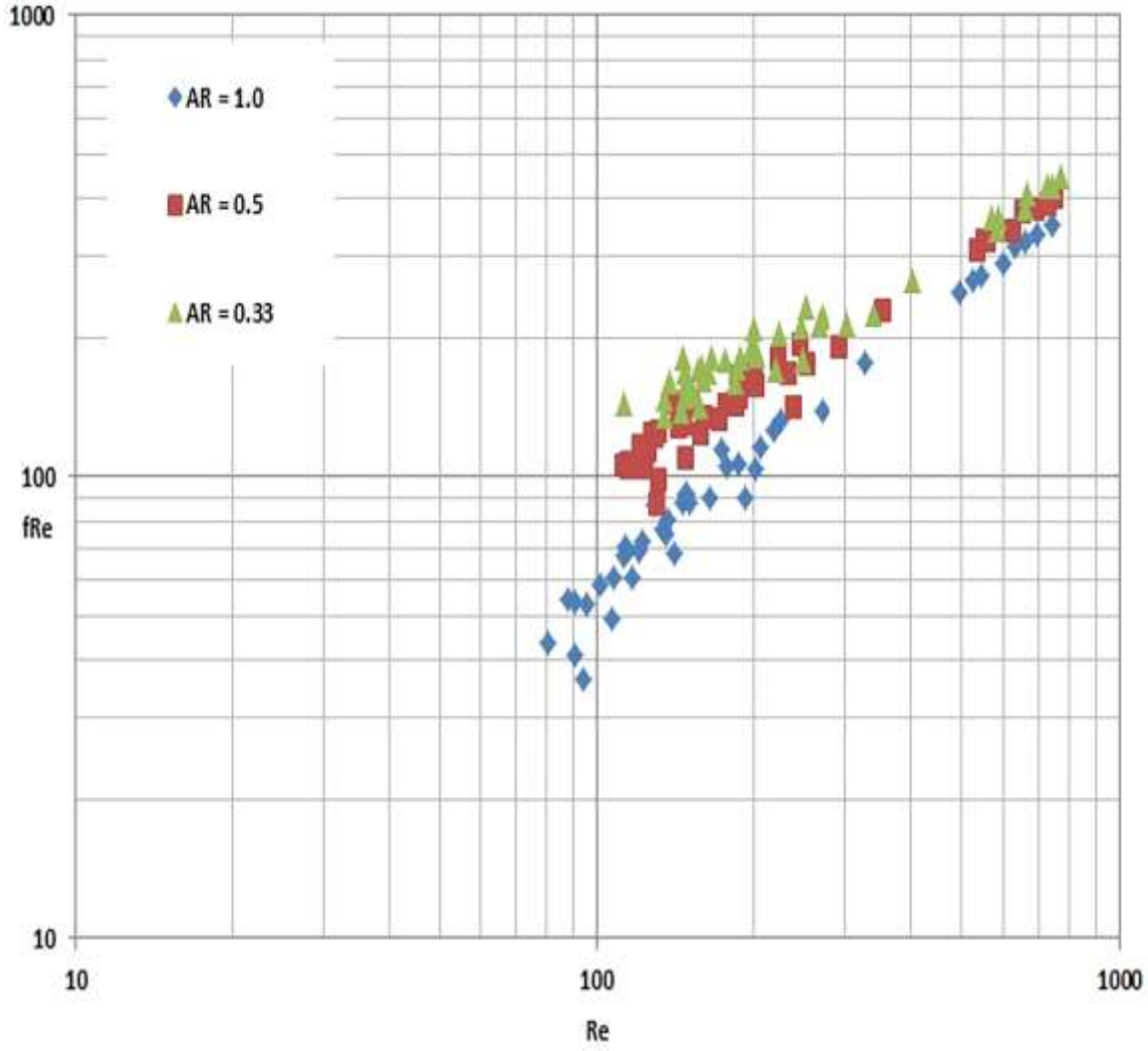

Fig. 12. Aspect ratio effect, twist ratio 2.5, tooth length 0.05263, tooth angle 30°, rib height 0.07894, rib pitch 20.

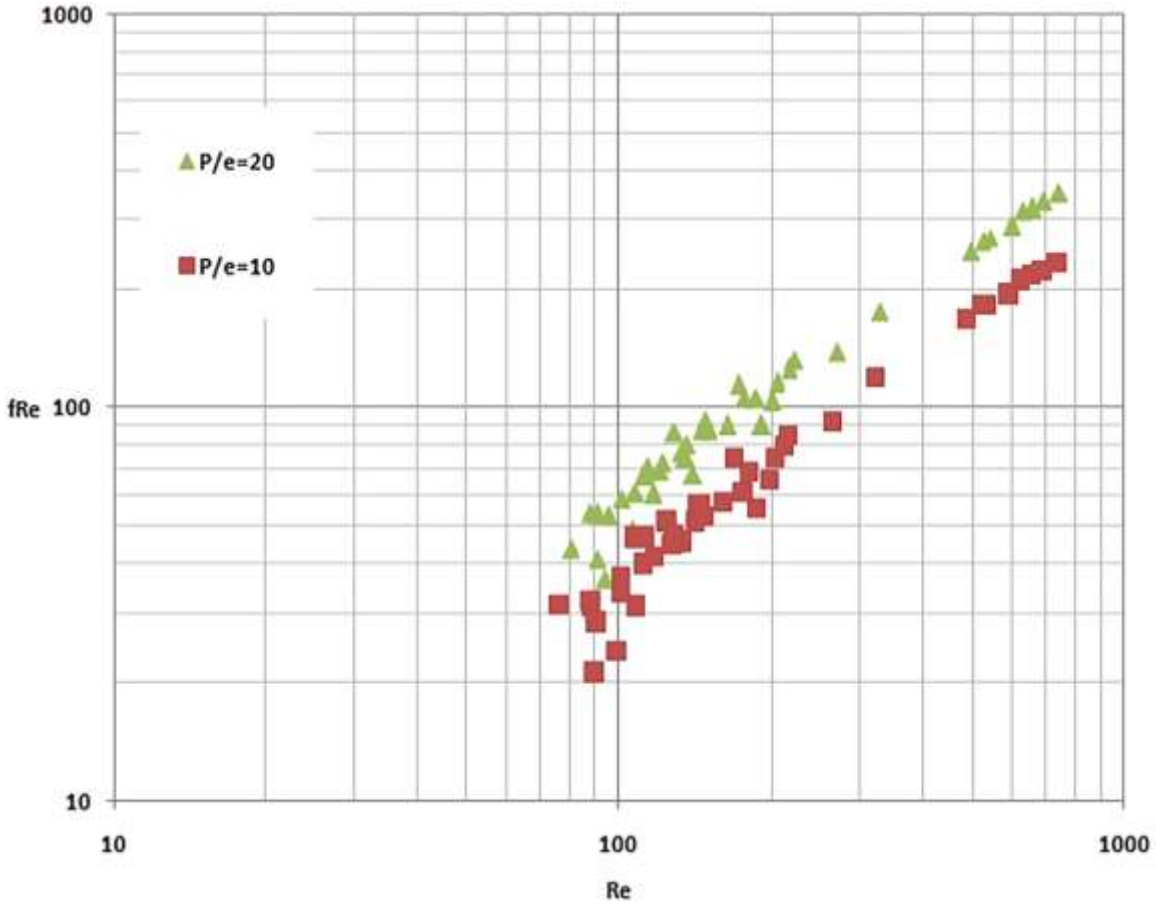

Fig. 13. Rib pitch effect, twist ratio 2.5, tooth length 0.05263, tooth angle 30°, rib height 0.07894, rib pitch 20.

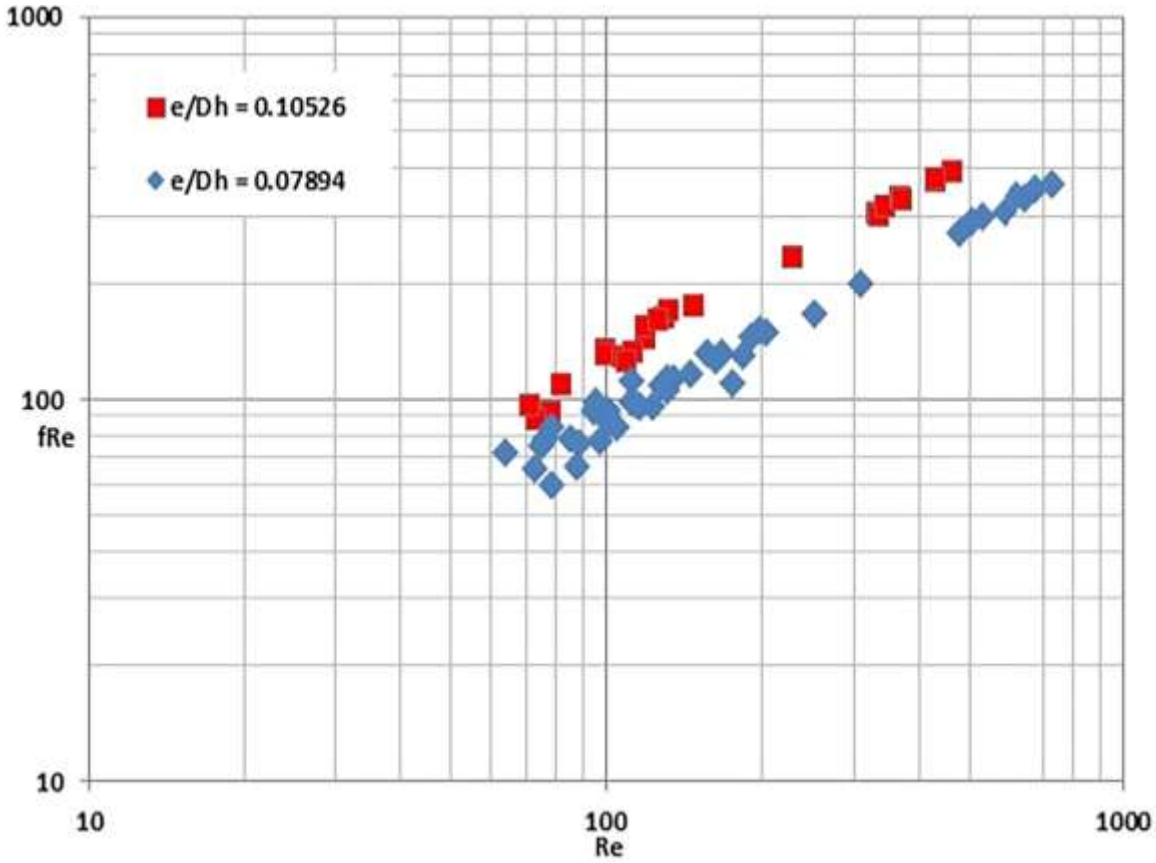

Fig. 14. Rib height effect, twist ratio 2.5, tooth length 0.1053, tooth angle 60°, rib pitch 10, aspect ratio 1.0.

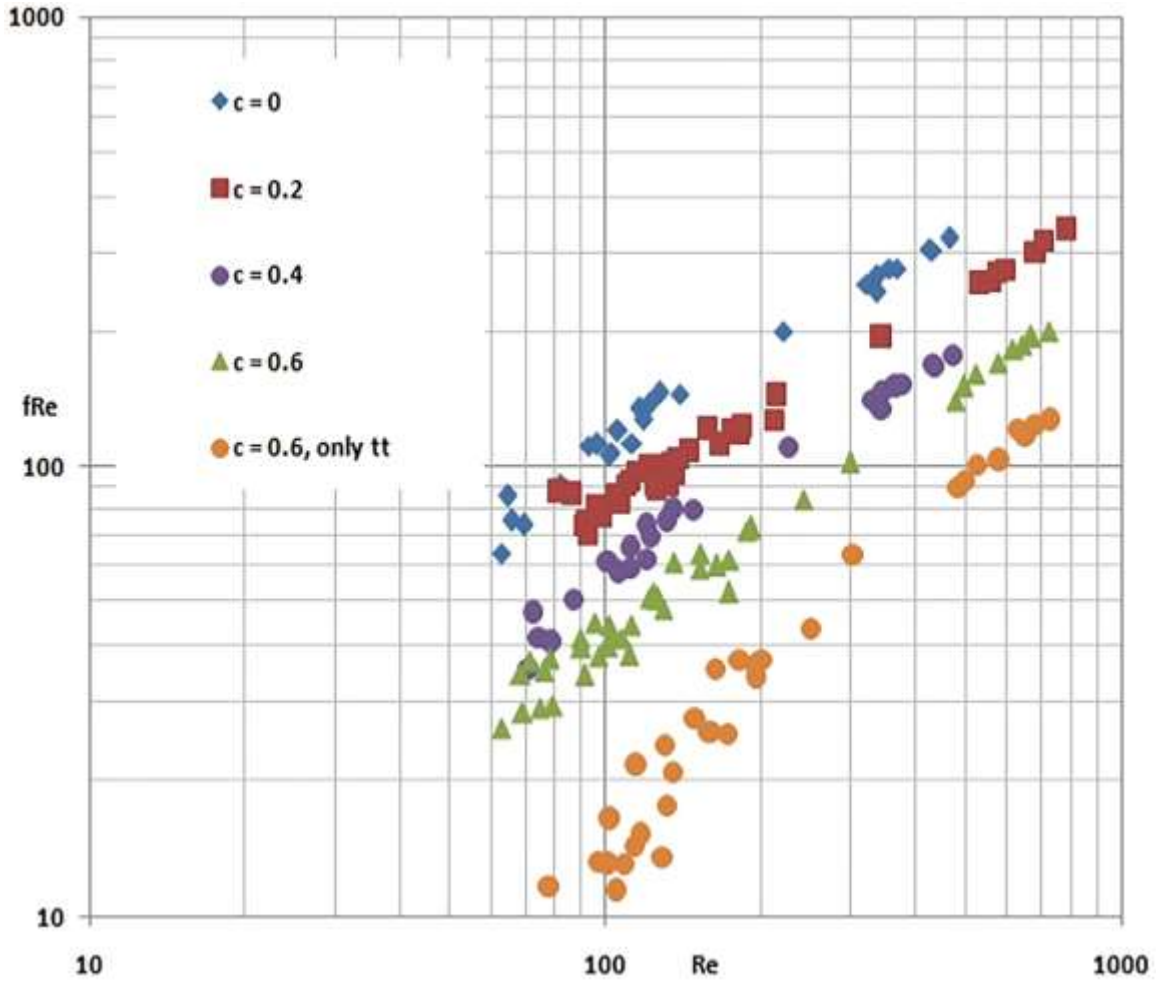

Fig. 15. Effect of centre-clearance of twisted-tape on friction factor: corrugation angle = 60°, corrugation pitch = 2.0437, aspect ratio = 1.0.

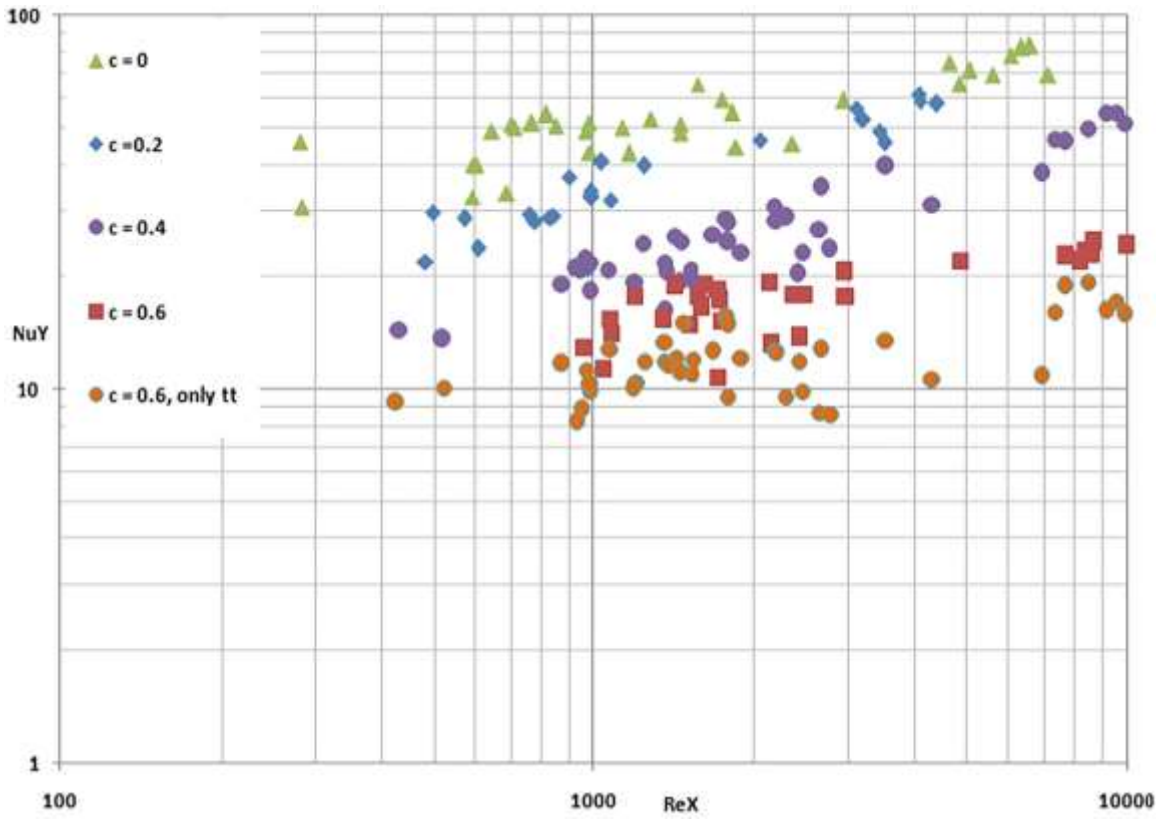

Fig. 16. Effect of centre clearance of twisted-tape on Nusselt number: corrugation angle = 60°, corrugation pitch = 2.0437, aspect ratio = 1.0.

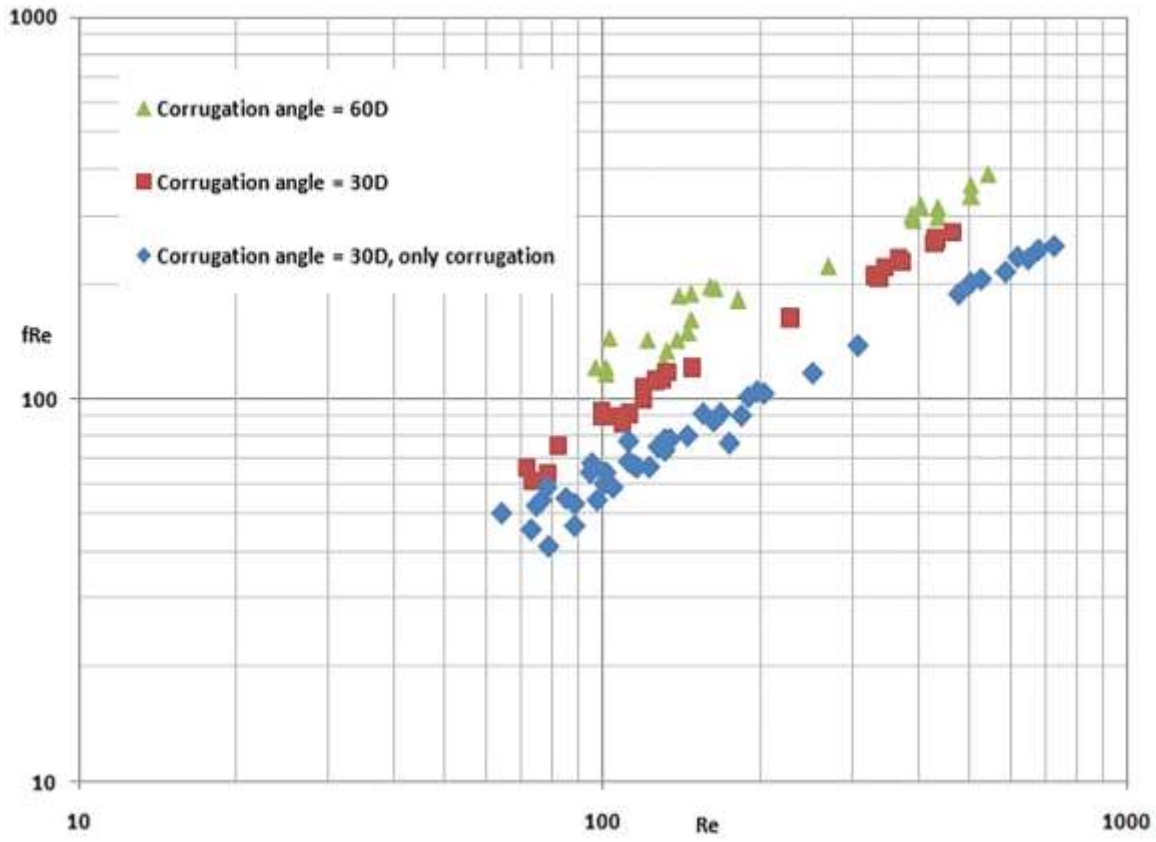

Fig. 17. Effect of corrugation angle on friction factor centre clearance = 0.4, corrugation pitch = 2.0437, aspect ratio = 1.0.

This was followed by the experiments with transverse rib and helical screw-tape inserts. The effect of fin parameters of helical screw-tape insert on friction factor and Nusselt number at fixed rib pitch and rib height is presented in Figure 18 and Figure 19, respectively for AR = 1.0. This trend of friction factor and Nusselt number was also found for aspect ratios 0.5 and 0.33. The aspect ratio trend is shown in Figure 20 at constant P/e = 2.0437, e/D_h = 0.07692 and p = infinity.

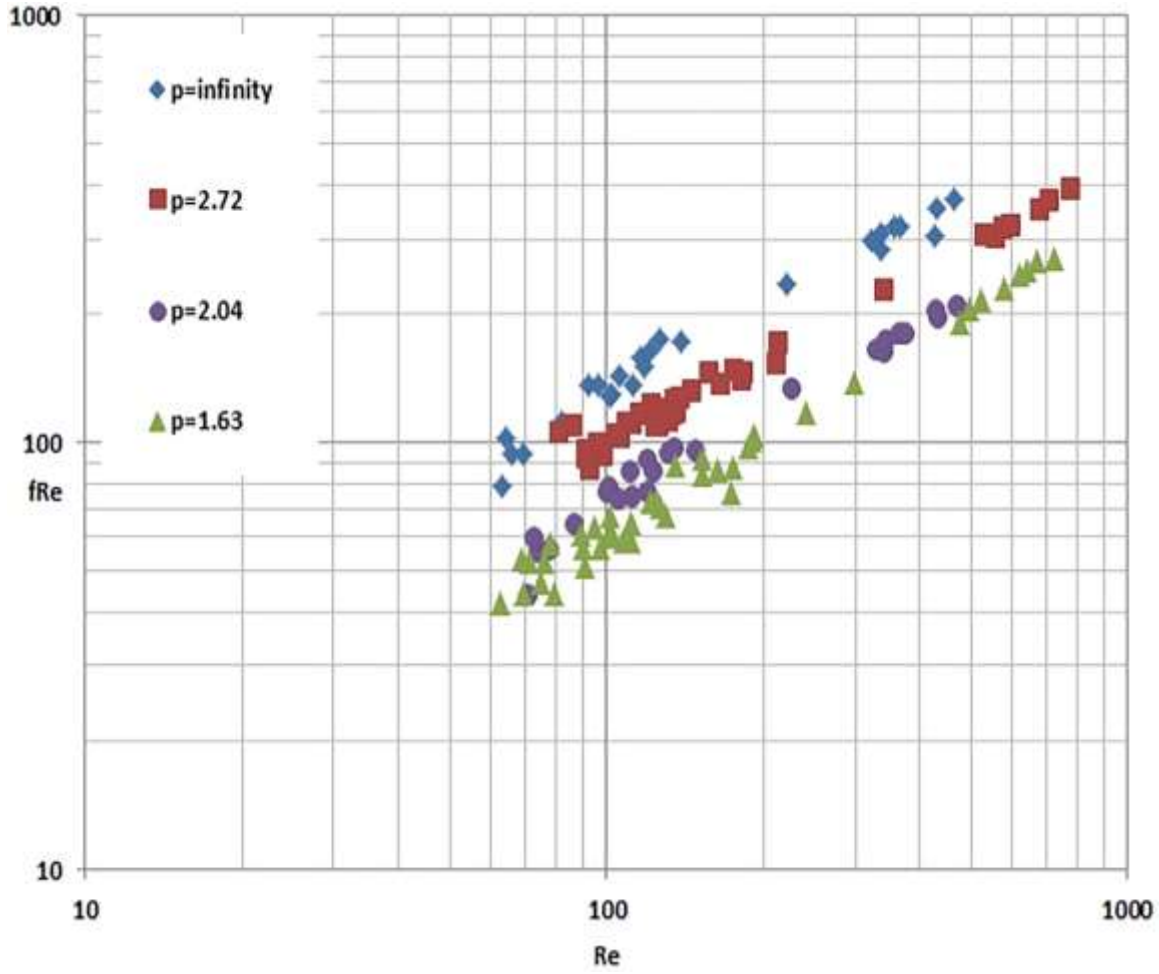

Fig. 18. Effect of fin parameter of helical screw-tape insert on friction factor: P/e = 2.0437, e/D_h = 0.07692, AR = 1.0.

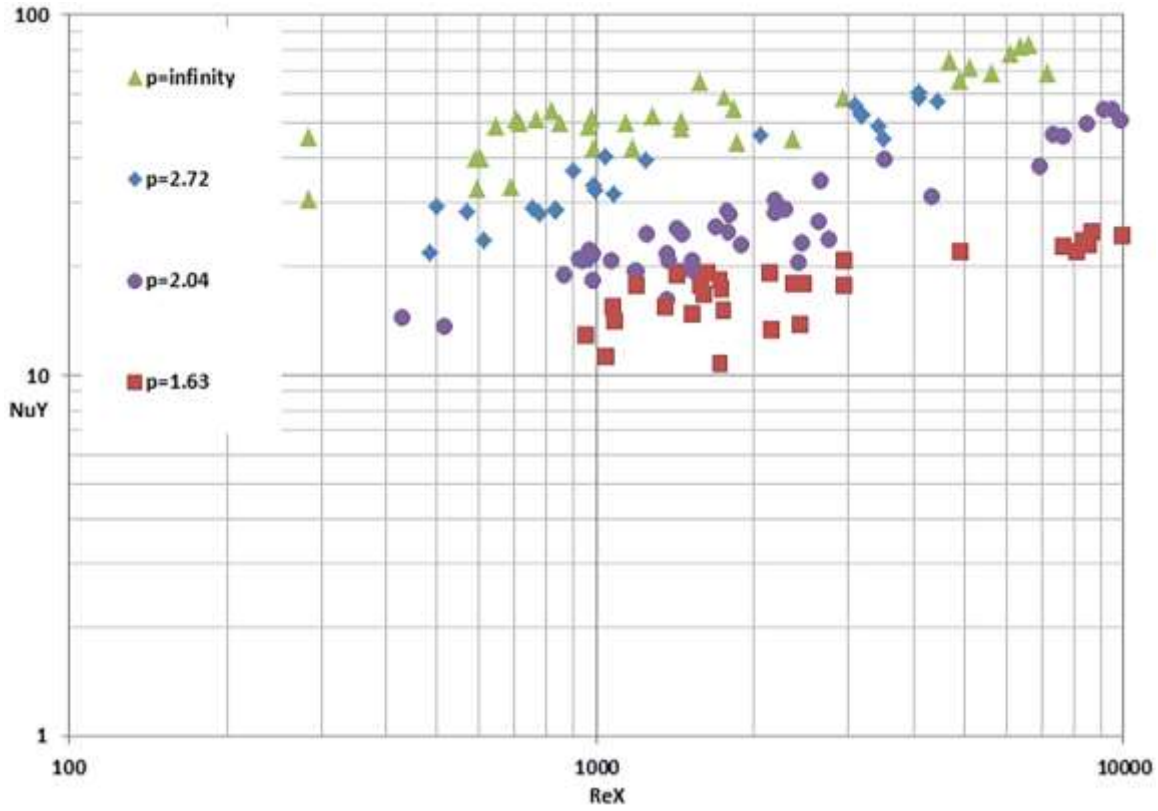

Fig. 19. Effect of fin parameter of helical screw-tape insert on Nusselt number: rib pitch = 2.0437, e/D_h = 0.1026, AR = 1.0.

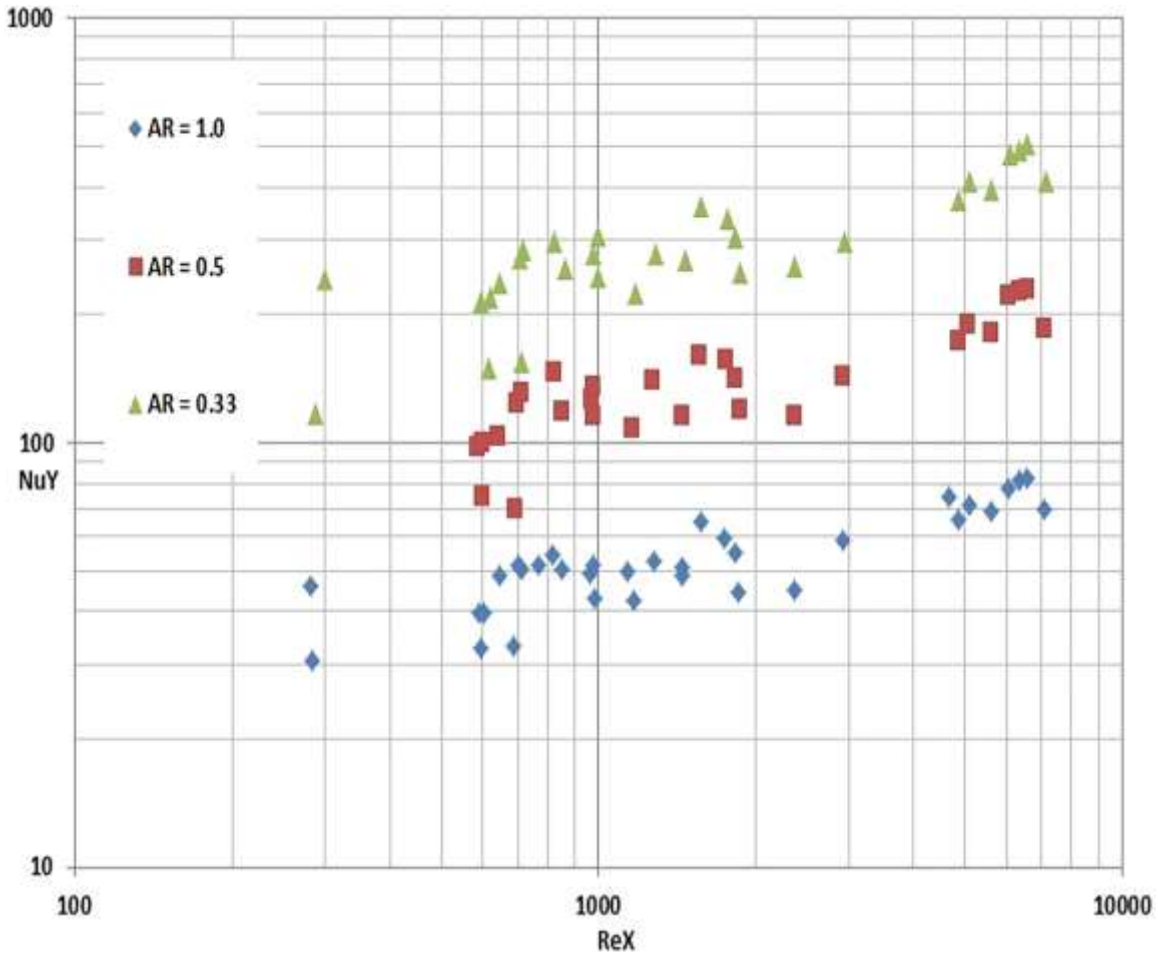

Fig. 20. Effect of aspect ratio on Nusselt number P/e = 2.0437,e/D_h = 0.07692, p= ∞.

The fourth set of experiments was done using axial rib with centre-cleared twisted-tape inserts. The axial rib is shown in Figure 3. The combined effects of axial rib and centre-cleared twisted-tape inserts on friction factor and Nusselt number are presented in Figure 21 and Figure 22, respectively. Only the twisted tape having centre clearance 0.4 had the least friction factor, whereas the twisted tape without centre clearance showed the maximum friction factor due to the maximum skin friction drag. The rib pitch effect on friction factor is shown in Figure 23. Friction factor decreased

with the decreasing rib pitch and it was the lowest when ribs were used for the heat transfer enhancement technique acting individually.

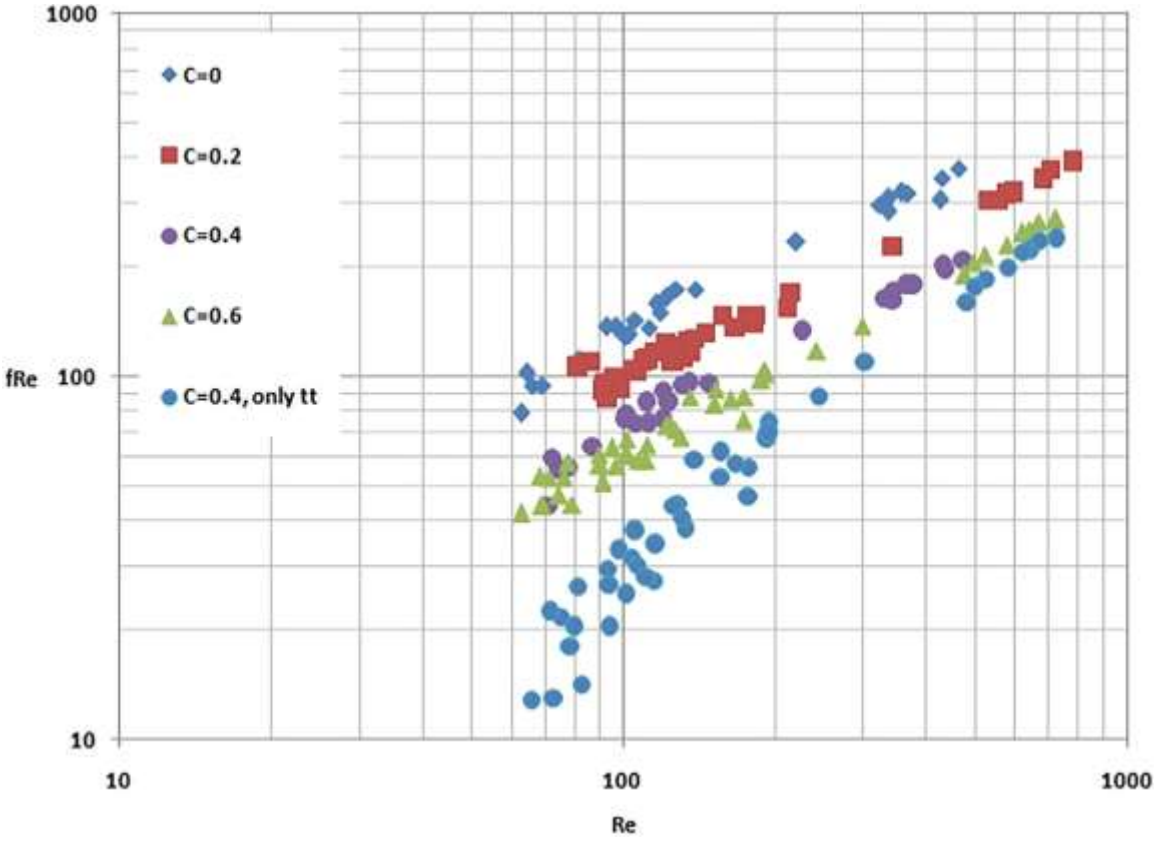

Fig. 21. Effect of centre clearance of twisted-tape on friction factor – P/e = 2.0437, e/D_h = 0.07692, AR = 1.0.

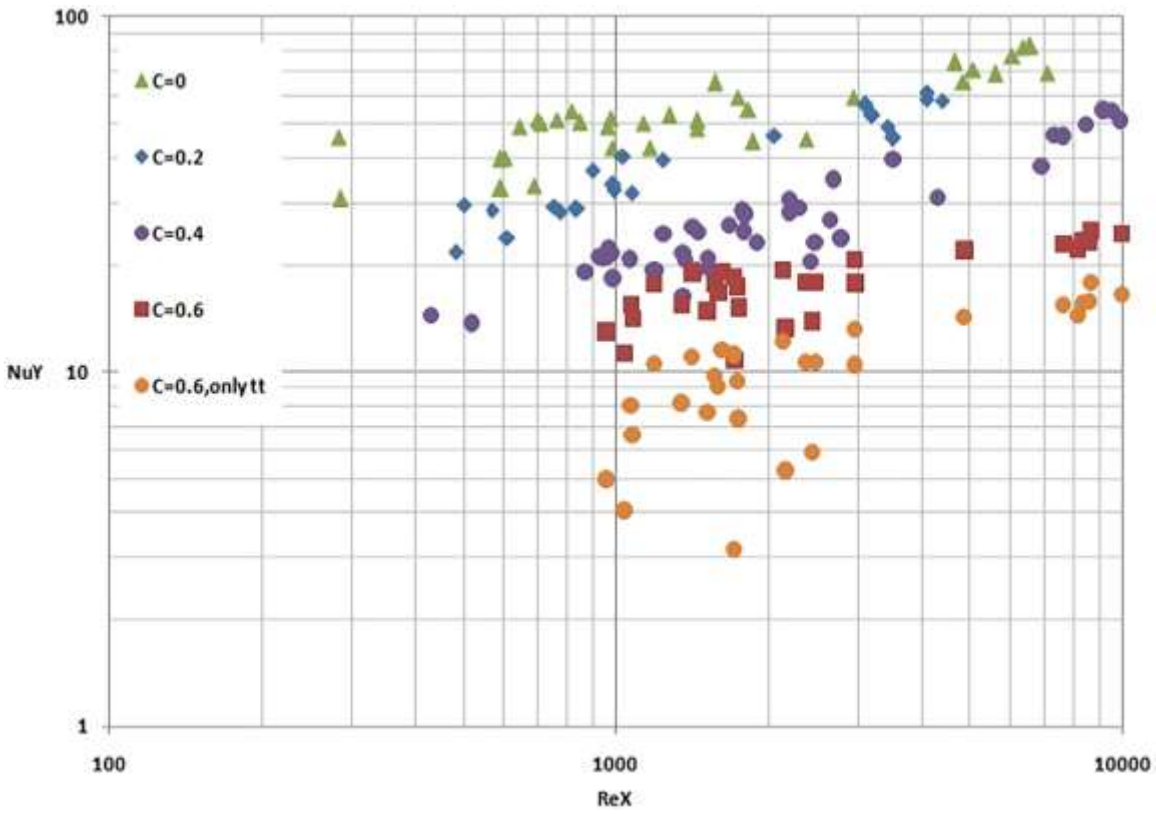

Fig. 22. Effect of centre clearance of twisted-tape on Nusselt number – rib pitch = 2.0437, e/D_h = 0.1026, AR = 1.0.

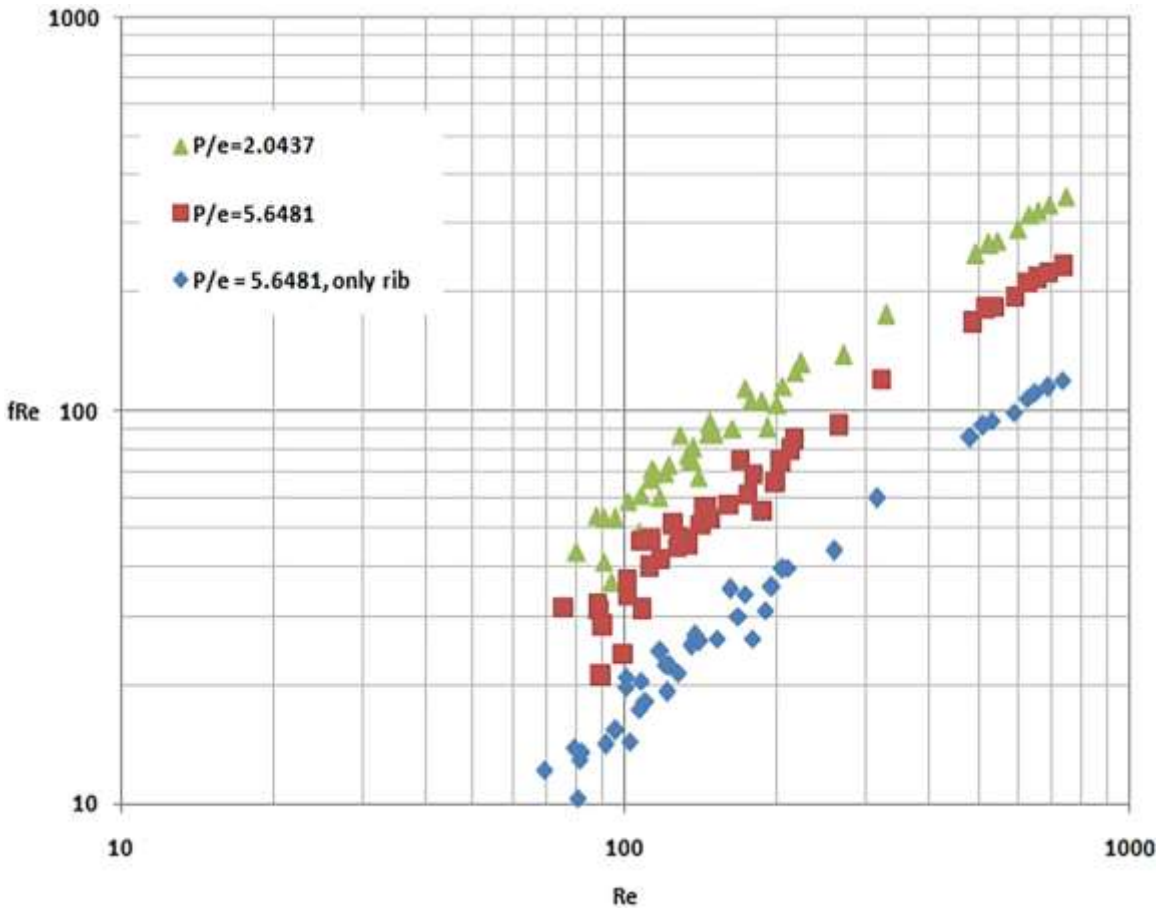

Fig. 23. Effect of rib pitch on friction factor – c = 0.4, e/D_h = 0.1026, AR = 1.0.

Finally, integral transverse rib roughness in combination with centre-cleared twisted-tape insert was examined. The effects of centre clearance on friction factor and Nusselt number are shown in Figure 24 and Figure 25, respectively. The resultant trend was similar to that of transverse corrugation with centre-cleared twisted-tape insert. The friction factor for zero centre clearance insert was maximum and for twisted-tape insert only with centre-clearance = 0.4, the data showed minimum friction factor and this trend was also seen in the Nusselt number vs Reynolds number plot. These

experimental observations could be plausibly explained phenomenologically by the boundary layer separation, flow reattachment, secondary flow and the fluid mixing.

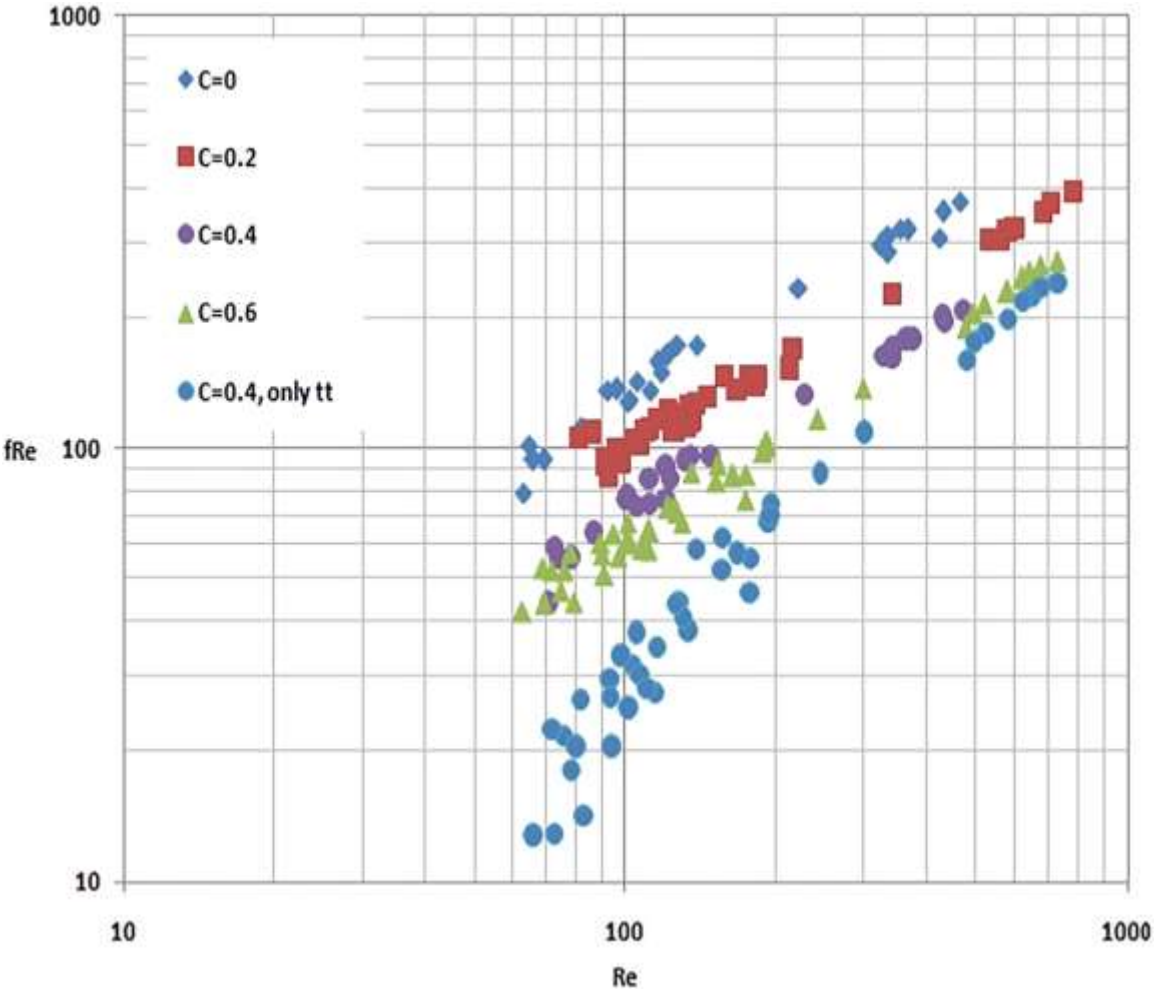

Fig. 24. Effect of centre clearance of twisted-tape on friction factor: P/e = 2.0437 and e/D_h = 0.07692, AR = 1.0.

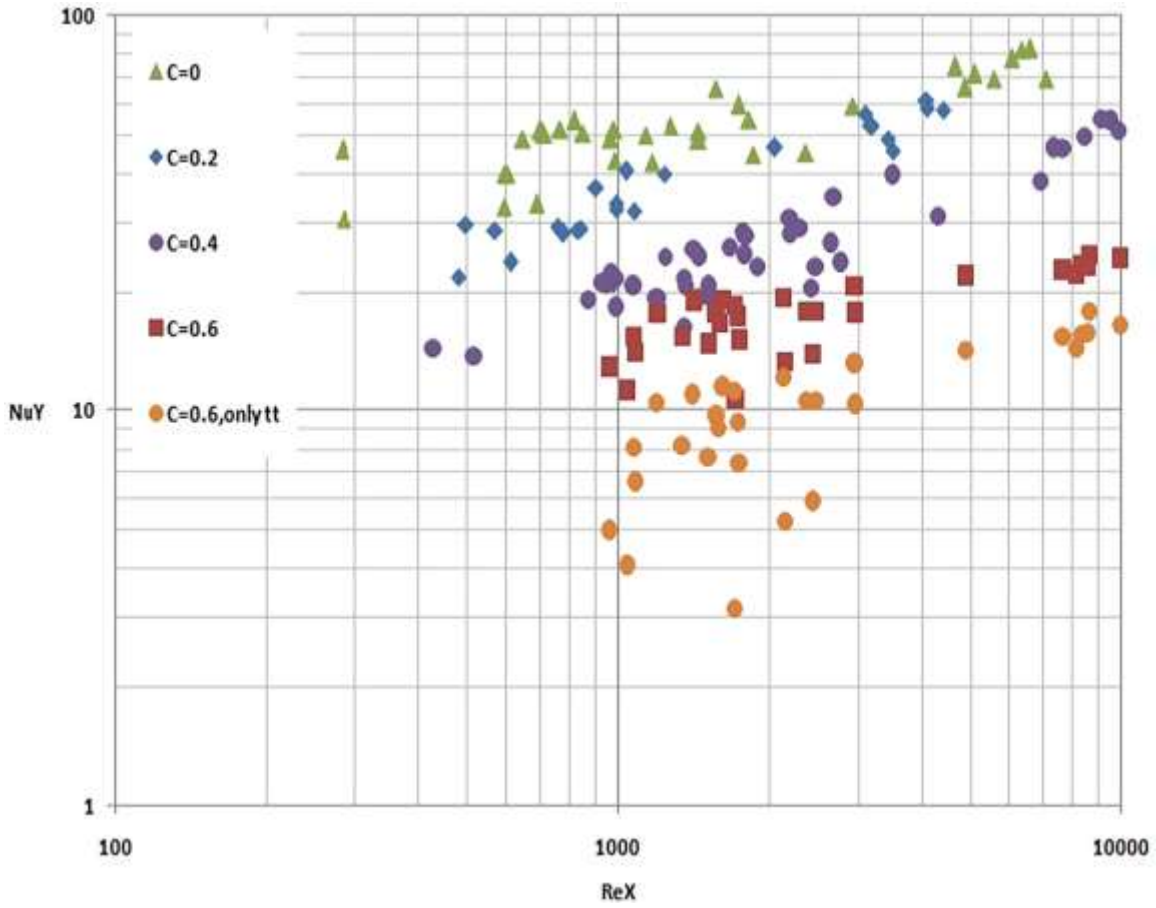

Fig. 25. Effect of centre clearance of twisted-tape on Nusselt number: rib pitch = 2.0437 and e/D_h = 0.1026, AR = 1.0.

4. CORRELATIONS

In this study, correlations for Nusselt number and friction factor for laminar flow through non-circular channels having combined transverse rib and twisted-tape inserts have been developed. Also, correlations for individual fins were established and these correlations could be very useful to professional engineers. The correlations predicted experimental data within ± 20 per cent. On an average, 85 per cent to 95 per cent data agreed very well with the correlations and the deviations were within $\pm$ 10 per cent.

The correlations for Nusselt number and friction factor for combined transverse rib and twisted-tape insert with oblique teeth are as follows:

$$Nu_{comb} = 5.172Gz^{0.279}\left(\frac{\mathrm{Re}}{\sqrt{y}}\right)^{0.132}\mathrm{Pr}^{0.5}\,Gr^{0.199}t_{hl}^{0.061}(\sin\theta)^{0.1228}\left(\frac{p}{e}\right)^{-0.717}\left(\frac{e}{D_h}\right)^{0.0821}\left(\frac{\mu_b}{\mu_w}\right)^{-0.138}\left(\frac{1}{AR}+0.1\right)^{0.153} \quad (1)$$

$$f\,\mathrm{Re}_{comb} = 81.7778\left(\frac{\mathrm{Re}}{\sqrt{y}}\right)^{0.458}t_{hl}^{0.033}(\sin\theta)^{0.028}\left(\frac{e}{D_h}\right)^{0.044}\left(\frac{p}{e}\right)^{-0.631}(AR)^{-1.235} \quad (2)$$

The correlations for the individual transverse ribs and twisted-tape insert with oblique teeth are as follows:

$$Nu = 5.172(Gz)^{0.137}(\mathrm{Re})^{0.347}\,\mathrm{Pr}^{0.422}\,Gr^{0.088}\left(\frac{p}{e}\right)^{-0.649}\left(\frac{e}{D_h}\right)^{0.026}\left(\frac{\mu_b}{\mu_w}\right)^{0.159}\left(\frac{1}{AR}+0.1\right)^{0.153} \quad (3)$$

$$f\,\mathrm{Re} = 23.4649(\mathrm{Re})^{0.508}\left(\frac{e}{D_h}\right)^{0.0247}\left(\frac{p}{e}\right)^{-0.535}(AR)^{-1.235} \quad (4)$$

$$Nu = 5.172Gz^{0.007}\left(\frac{\mathrm{Re}}{\sqrt{y}}\right)^{0.389}\mathrm{Pr}^{0.155}\,Gr^{0.026}t_{hl}^{0.159}(\sin\theta)^{0.109}\left(\frac{\mu_b}{\mu_w}\right)^{-0.138}\left(\frac{1}{AR}+0.1\right)^{0.153} \quad (5)$$

$$f\,\mathrm{Re} = 65.1927\left(\frac{\mathrm{Re}}{\sqrt{y}}\right)^{0.264}t_{hl}^{0.071}(\sin\theta)^{0.255}(AR)^{-1.235} \quad (6)$$

Similarly, the correlations for Nusselt number for a combination of integral transverse corrugation and centre-cleared twisted-tape insert are given by:

$$Nu_m = 5.174\left[\left(\left(1+0.0711Gz^{0.895}\right)^{2.52} + 8.314\times10^{-6}\left(Sw.\Pr^{0.565}\right)^{2.623}\right)^{2.0} + 1.5114\times10^{-14}\left(\mathrm{Re}_{ax.}\,Ra\right)^{2.17}\right]^{0.1}$$
$$\times\left(\mu_b/\mu_w\right)^{0.14}\left(\frac{1}{AR}+0.1\right)^{0.153}\times\left(1+\frac{\left(1+\exp\left(0.0888822c\right)\right)\times\exp\left(0.07399\sin\theta\right)}{\left(P/e\right)^{0.652}}\right) \quad (7)$$

And friction factor for the above combination is presented as:

$$\left(f\,\mathrm{Re}\right)_{sw} = 17.351\left(\frac{\Pi+2-\frac{2t}{D_h}}{\left(\frac{\Pi-4t}{D_h}\right)}\right)^{2.01}\left(1+10^{-6}\,Sw^{2.645}\right)^{0.14}\times$$
$$\left(1+\frac{\left(1+\exp\left(0.088c\right)\right)\times\exp\left(0.06987\sin\theta\right)}{\left(\frac{P}{e}\right)^{0.654}}\right) \quad (8)$$

The correlation for Nusselt number for the transverse rib and helical screw-tape insert combination is:

$$Nu_m = 5.174\left[\begin{matrix}\left(\left(1+0.074966Gz^{0.8452}\right)^{2.5565}+8.46523\times10^{-6}\left(Sw.\Pr^{0.54969}\right)^{2.6694}\right)^{2.0}+\\ 1.5049523\times10^{-15}\left(\mathrm{Re}_{ax.}\,Ra\right)^{2.16}\end{matrix}\right]^{0.1}$$
$$\times\left(\mu_b/\mu_w\right)^{0.14}\left(\frac{1}{AR}+0.1\right)^{0.153}\times\left(1+\frac{\left(1+\exp\left(0.08794526p\right)\right)\times\left(\frac{e}{D_h}\right)^{0.625754}}{\left(P/e\right)^{0.6458}}\right) \quad (9)$$

and friction factor for this combination is:

$$\left(f\,\mathrm{Re}\right)_{sw} = 17.351\left(\frac{\Pi+2-\frac{2t}{D_h}}{\left(\frac{\Pi-4t}{D_h}\right)}\right)^{2.01}\left(1+10^{-6}\,Sw^{2.6801}\right)^{0.141}1\times\left(1+\frac{\left(1+\exp\left(0.083p\right)\right)\times\left(\frac{e}{D_h}\right)^{0.625754}}{\left(\frac{P}{e}\right)^{0.625754}}\right)$$
$$\left(AR\right)^{-1.235} \quad (10)$$

The correlation for Nusselt number for combined axial rib and centre-cleared twisted tape is:

$$Nu_m = 5.170\left[\begin{array}{l}\left(\left(1+0.070511Gz^{0.88952}\right)^{2.552}+8.02314\times10^{-6}\left(Sw.\Pr^{0.565}\right)^{2.6523}\right)^{2.0}+\\ 1.52114\times10^{-15}\left(\mathrm{Re}_{ax.}\,Ra\right)^{2.179}\end{array}\right]^{0.1}$$
$$\times\left(\mu_b/\mu_w\right)^{0.14}\left(\frac{1}{AR}+0.1\right)^{0.153}\times\left(1+\frac{\left(1+\exp\left(0.099822c\right)\right)\times\left(\frac{e}{D_h}\right)^{0.06547}}{\left(P/e\right)^{0.746452}}\right) \quad (11)$$

and friction factor for the present combination is given by:

$$\left(f\,\mathrm{Re}\right)_{sw} = 17.351\left(\frac{\Pi+2-\frac{2t}{D_h}}{\left(\frac{\Pi-4t}{D_h}\right)}\right)^{2.01}\left(1+10^{-6}\,Sw^{2.645}\right)^{0.14}\times\left(1+\frac{\left(1+\exp\left(0.088c\right)\right)\times\left(\frac{e}{D_h}\right)^{0.06547}}{\left(\frac{P}{e}\right)^{0.74645}}\right) \quad (12)$$
$$\left(AR\right)^{-1.235}$$

Nusselt number and friction factor correlations for combined transverse rib and centre-cleared twisted-tape insert are as follows:

$$Nu_m = 5.170\left[\begin{array}{l}\left(\left(1+0.070511Gz^{0.88952}\right)^{2.552}+8.02314\times10^{-6}\left(Sw.\Pr^{0.565}\right)^{2.6523}\right)^{2.0}+\\ 1.52114\times10^{-15}\left(\mathrm{Re}_{ax.}\,Ra\right)^{2.179}\end{array}\right]^{0.1}$$
$$\times\left(\mu_b/\mu_w\right)^{0.14}\left(\frac{1}{AR}+0.1\right)^{0.153}\times\left(1+\frac{\left(1+\exp\left(0.099822c\right)\right)\times\left(\frac{e}{D_h}\right)^{0.05444521}}{\left(P/e\right)^{0.746452}}\right) \quad (13)$$

$$\left(f\,\mathrm{Re}\right)_{sw} = 17.351\left(\frac{\Pi+2-\frac{2t}{D_h}}{\left(\frac{\Pi-4t}{D_h}\right)}\right)^{2.01}\left(1+10^{-6}\,Sw^{2.645}\right)^{0.14}\times\left(1+\frac{\left(1+\exp\left(0.088c\right)\right)\times\left(\frac{e}{D_h}\right)^{0.44521}}{\left(\frac{P}{e}\right)^{0.61254}}\right) \quad (14)$$
$$\left(AR\right)^{-1.235}$$

5. PERFORMANCE EVALUATION

Performance evaluation is necessary for finding the best best fin geometry configuration. There are two standard methods for performance evaluation [35]:

$P_1=\frac{enhancedgeometry}{non-enhancedgeometry}$, for increased thermal energy transport and fixed pumping power;

$P_2=\frac{enhancedgeometry}{non-enhancedgeometry}$, for constant heat duty and reduced pumping power.

$P_1 > 1$ and $P_2 < 1$ are useful for fin geometry and these are recommended for use in the industry.

A performance evaluation of transverse rib and twisted tape with oblique teeth combination is presented in Table 1 and Table 2 with parameters $P_1$and P_2, respectively. Similarly, a performance evaluation for integral transverse corrugations with centre-cleared twisted-tape inserts is presented in Table 3 and Table 4 with parameters P_1 and P_2 ,respectively. The Tables and fin geometry studies should be useful for industrial application and the correlations could be used in designing heat exchangers.

There is no information in the open literature with which to compare the present results. Standard results were used for the validation of the rig.

Table 1 Performance evaluation of combined transverse rib and oblique twisted tape at parameter P_1

P_1								
AR 1.0	**R2R2**		**R1R2**		**R2R1**		**R1R1**	
t_{h1} = 0.05263, θ = 30°	P_{R1R1}	P_{R1R2}	P_{R1R1}	P_{R1R2}	P_{R1R1}	P_{R1R2}	P_{R1R1}	P_{R1R2}
	1.663	**1.677**	**1.701**	**1.713**	**1.731**	**1.746**	**1.758**	**1.769**
t_{h1} = 0.1053, θ = 30°	P_{R1R1}	P_{R1R2}	P_{R1R1}	P_{R1R2}	P_{R1R1}	P_{R1R2}	P_{R1R1}	P_{R1R2}
	1.666	**1.689**	**1.693**	**1.696**	**1.703**	**1.703**	**1.720**	**1.730**
t_{h1} = 0.05263, θ = 60°	P_{R1R1}	P_{R1R2}	P_{R1R1}	P_{R1R2}	P_{R1R1}	P_{R1R2}	P_{R1R1}	P_{R1R2}
	1.570	**1.581**	**1.583**	**1.591**	**1.615**	**1.639**	**1.659**	**1.681**
t_{h1} = 0.1053, θ = 60°	P_{R1R1}	P_{R1R2}	P_{R1R1}	P_{R1R2}	P_{R1R1}	P_{R1R2}	P_{R1R1}	P_{R1R2}
	1.620	**1.643**	**1.655**	**1.677**	**1.694**	**1.697**	**1.7R1R1**	**1.713**

P_1								
AR 0.5	**R2R2**		**R1R2**		**R2R1**		**R1R1**	
t_{h1} = 0.05263, θ = 30°	P_{R1R1}	P_{R1R2}	P_{R1R1}	P_{R1R2}	P_{R1R1}	P_{R1R2}	P_{R1R1}	P_{R1R2}
	1.652	**1.655**	**1.670**	**1.680**	**1.687**	**1.703**	**1.712**	**1.729**
t_{h1} = 0.1053, θ = 30°	P_{R1R1}	P_{R1R2}	P_{R1R1}	P_{R1R2}	P_{R1R1}	P_{R1R2}	P_{R1R1}	P_{R1R2}
	1.673	**1.686**	**1.689**	**1.710**	**1.732**	**1.733**	**1.753**	**1.756**
t_{h1} = 0.05263, θ = 60°	P_{R1R1}	P_{R1R2}	P_{R1R1}	P_{R1R2}	P_{R1R1}	P_{R1R2}	P_{R1R1}	P_{R1R2}
	1.553	**1.565**	**1.572**	**1.585**	**1.585**	**1.596**	**1.609**	**1.613**
t_{h1} = 0.1053, θ = 60°	P_{R1R1}	P_{R1R2}	P_{R1R1}	P_{R1R2}	P_{R1R1}	P_{R1R2}	P_{R1R1}	P_{R1R2}
	1.613	**1.615**	**1.633**	**1.643**	**1.644**	**1.658**	**1.680**	**1.680**

P_1								
AR 0.33	**R2R2**		**R1R2**		**R2R1**		**R1R1**	
t_{h1} = 0.05263, θ = 30°	P_{R1R1}	P_{R1R2}	P_{R1R1}	P_{R1R2}	P_{R1R1}	P_{R1R2}	P_{R1R1}	P_{R1R2}
	1.656	**1.677**	**1.681**	**1.694**	**1.700**	**1.713**	**1.737**	**1.755**
t_{h1} = 0.1053, θ = 30°	P_{R1R1}	P_{R1R2}	P_{R1R1}	P_{R1R2}	P_{R1R1}	P_{R1R2}	P_{R1R1}	P_{R1R2}
	1.671	**1.684**	**1.701**	**1.719**	**1.730**	**1.740**	**1.740**	**1.753**

t_{h1} = 0.05263, θ = 60°	P_{R1R1}	P_{R1R2}	P_{R1R1}	P_{R1R2}	P_{R1R1}	P_{R1R2}	P_{R1R1}	P_{R1R2}
	1.569	**1.590**	**1.609**	**1.632**	**1.638**	**1.640**	**1.659**	**1.679**
t_{h1} = 0.1053, θ = 60°	P_{R1R1}	P_{R1R2}	P_{R1R1}	P_{R1R2}	P_{R1R1}	P_{R1R2}	P_{R1R1}	P_{R1R2}
	1.600	**1.621**	**1.633**	**1.646**	**1.660**	**1.662**	**1.671**	**1.674**

Table 2 Performance evaluationof transverse rib and twisted tape with oblique teeth at parameter P_2

P_2								
AR 1.0	**R2R2**		**R1R2**		**R2R1**		**R1R1**	
t_{h1} = 0.05263, θ = 30°	P_{R2R1}	P_{R2R2}	P_{R2R1}	P_{R2R2}	P_{R2R1}	P_{R2R2}	P_{R2R1}	P_{R2R2}
	0.767	**0.768**	**0.770**	**0.772**	**0.772**	**0.772**	**0.774**	**0.774**
t_{h1} = 0.1053, θ = 30°	P_{R2R1}	P_{R2R2}	P_{R2R1}	P_{R2R2}	P_{R2R1}	P_{R2R2}	P_{R2R1}	P_{R2R2}
	0.766	**0.767**	**0.770**	**0.771**	**0.771**	**0.773**	**0.774**	**0.775**
t_{h1} = 0.05263, θ = 60°	P_{R2R1}	P_{R2R2}	P_{R2R1}	P_{R2R2}	P_{R2R1}	P_{R2R2}	P_{R2R1}	P_{R2R2}
	0.750	**0.752**	**0.753**	**0.755**	**0.757**	**0.758**	**0.758**	**0.759**
t_{h1} = 0.1053, θ = 60°	P_{R2R1}	P_{R2R2}	P_{R2R1}	P_{R2R2}	P_{R2R1}	P_{R2R2}	P_{R2R1}	P_{R2R2}
	0.675	**0.675**	**0.677**	**0.679**	**0.680**	**0.683**	**0.684**	**0.684**

P_2								
AR 0.5	**R2R2**		**R1R2**		**R2R1**		**R1R1**	
t_{h1} = 0.05263, θ = 30°	P_{R2R1}	P_{R2R2}	P_{R2R1}	P_{R2R2}	P_{R2R1}	P_{R2R2}	P_{R2R1}	P_{R2R2}
	0.766	**0.766**	**0.768**	**0.770**	**0.770**	**0.773**	**0.774**	**0.774**
t_{h1} = 0.1053, θ = 30°	P_{R2R1}	P_{R2R2}	P_{R2R1}	P_{R2R2}	P_{R2R1}	P_{R2R2}	P_{R2R1}	P_{R2R2}
	0.767	**0.767**	**0.768**	**0.768**	**0.770**	**0.771**	**0.773**	**0.773**
t_{h1} = 0.05263, θ = 60°	P_{R2R1}	P_{R2R2}	P_{R2R1}	P_{R2R2}	P_{R2R1}	P_{R2R2}	P_{R2R1}	P_{R2R2}
	0.751	**0.753**	**0.755**	**0.756**	**0.758**	**0.759**	**0.761**	**0.763**
t_{h1} = 0.1053, θ = 60°	P_{R2R1}	P_{R2R2}	P_{R2R1}	P_{R2R2}	P_{R2R1}	P_{R2R2}	P_{R2R1}	P_{R2R2}
	0.674	**0.675**	**0.676**	**0.677**	**0.677**	**0.680**	**0.681**	**0.683**

P_2								
AR 0.33	**R2R2**		**R1R2**		**R2R1**		**R1R1**	
t_{h1} = 0.05263, θ = 30°	P_{R2R1}	P_{R2R2}	P_{R2R1}	P_{R2R2}	P_{R2R1}	P_{R2R2}	P_{R2R1}	P_{R2R2}
	0.768	**0.769**	**0.771**	**0.773**	**0.774**	**0.774**	**0.776**	**0.778**
t_{h1} = 0.1053, θ = 30°	P_{R2R1}	P_{R2R2}	P_{R2R1}	P_{R2R2}	P_{R2R1}	P_{R2R2}	P_{R2R1}	P_{R2R2}

	0.768	**0.768**	**0.769**	**0.769**	**0.770**	**0.772**	**0.772**	**0.772**
t_{h1} = 0.05263, θ = 60°	P_{R2R1}	P_{R2R2}	P_{R2R1}	P_{R2R2}	P_{R2R1}	P_{R2R2}	P_{R2R1}	P_{R2R2}
	0.751	**0.752**	**0.752**	**0.753**	**0.755**	**0.756**	**0.757**	**0.758**
t_{h1} = 0.1053, θ = 60°	P_{R2R1}	P_{R2R2}	P_{R2R1}	P_{R2R2}	P_{R2R1}	P_{R2R2}	P_{R2R1}	P_{R2R2}
	0.675	**0.676**	**0.677**	**0.678**	**0.679**	**0.681**	**0.683**	**0.684**

Table 3 Performance evaluation of transverse corrugations and centre-cleared twisted tape at parameter P_1

P_1				
AR 1.0				
	R2R2	**R1R2**	**R2R1**	**R1R1**
c = 0.2	**1.498**	**1.637**	**1.659**	**1.764**
c = 0.4	**1.780**	**1.626**	**1.628**	**1.744**
c = 0.6	**1.626**	**1.723**	**1.734**	**1.459**
AR 0.5				
	R2R2	**R1R2**	**R2R1**	**R1R1**
c = 0.2	**1.646**	**1.804**	**1.739**	**1.650**
c = 0.4	**1.670**	**1.807**	**1.808**	**1.799**
c = 0.6	**1.716**	**1.670**	**1.604**	**1.716**
AR 0.33				
	R2R2	**R1R2**	**R2R1**	**R1R1**
c = 0.2	**1.818**	**1.699**	**1.687**	**1.775**
c = 0.4	**1.816**	**1.682**	**1.779**	**1.789**
c = 0.6	**1.788**	**1.664**	**1.946**	**1.670**
Circular Duct				
	R2R2	**R1R2**	**R2R1**	**R1R1**
c = 0.2	**1.651**	**1.608**	**1.735**	**1.604**
c = 0.4	**1.732**	**1.543**	**1.799**	**1.749**
c = 0.6	**1.789**	**1.707**	**1.754**	**1.758**

Table 4 Performance evaluation of transverse corrugations and centre-cleared twisted tape at parameter P_2

P_2				
AR 1.0				
	R2R2	**R1R2**	**R2R1**	**R1R1**
c = 0.2	**0.796**	**0.702**	**0.739**	**0.759**
c = 0.4	**0.772**	**0.668**	**0.650**	**0.663**
c = 0.6	**0.756**	**0.655**	**0.665**	**0.666**
AR 0.5				
	R2R2	**R1R2**	**R2R1**	**R1R1**
c = 0.2	**0.730**	**0.708**	**0.717**	**0.714**
c = 0.4	**0.651**	**0.620**	**0.628**	**0.640**
c = 0.6	**0.663**	**0.656**	**0.650**	**0.649**
AR 0.33				
	R2R2	**R1R2**	**R2R1**	**R1R1**
c = 0.2	**0.723**	**0.712**	**0.698**	**0.677**
c = 0.4	**0.611**	**0.615**	**0.617**	**0.608**
c = 0.6	**0.631**	**0.622**	**0.614**	**0.599**
Circular Duct				
	R2R2	**R1R2**	**R2R1**	**R1R1**
c = 0.2	**0.689**	**0.680**	**0.648**	**0.679**
c = 0.4	**0.606**	**0.620**	**0.606**	**0.568**
c = 0.6	**0.605**	**0.598**	**0.595**	**0.632**

6. CONCLUSIONS

The following conclusions are drawn from the experimental investigation:

- The friction factor and Nusselt number are higher than those of the plain tube and the performance of combined inserts is better than that of the individual technique.
- The performance of the combination was better than that of individual inserts of all kinds. It is concluded from the present investigation that 31-52 per cent

increase in heat duty at constant pumping power and 25-36 per cent reduction in pumping power at constant heat duty are achievable. This is the novelty of the present work since no such study and the observations were made earlier. These types of combined fin configurations have not been tried before.

- Friction factor and Nusselt number correlations are presented for various combinations as well as for individual inserts.
- The hydrothermal performance is evaluated for the combined use of five different enhancement techniques: (1) transverse ribs with twisted-tape insert with oblique teeth, (2) integral transverse corrugation and centre-cleared twisted-tape insert, (3) transverse rib and helical screw-tape insert, (4) axial ribs and centre-cleared twisted-tape insert and (5) integral transverse rib and centre-cleared twisted-tape insert. Such investigations are unique and never tried before, These findings are very useful in industry.
- The results of various combinations of inserts are presented and these are useful for industrial purposes. The findings are likely to have good impact in the industry.

ACKNOWLEDEGMENT

Financial support for the current research from AICTE [20/AICTE/RIFD/RPS (Policy II): 84/2012-2013]; UGC [UGC 41-989/2012 (SR)]; DST [SR/S3/MERC-0045/2010(G)],CSIR [22(0386)/05/EMR-II]and the Government of India is gratefully acknowledged.

NOMENCLATURE

A	heat transfer area, m^2
A_c	axial flow cross-sectional area, m^2
A_o	plain duct flow cross-sectional area, m^2
C	twisted-tape centre-clearance, m
c	non-dimensional twisted-tape centre-clearance, dimensionless
c_p	constant pressure specific heat, J/kg k
D	internal diameter of the plain duct, m
D_h	hydraulic diameter of the test duct, m
d	helical screw-tape rod diameter, m
e	rib height, corrugation height, m
f	fully developed Fanning friction factor, dimensionless
f_{sw}	swirl flow friction factor, dimensionless
g	gravitational acceleration, m/s^2
Gr	Grashoff number, dimensionless
Gz	Graetz number, dimensionless
H	pitch for 180^0 rotation of twisted-tape, m
h_z	axial local heat transfer coefficient, $W/(m^2K)$
k	fluid thermal conductivity, W/(mK)
L_s	maximum helical flow length, m

l	non-dimensional twisted-tape length, dimensionless
θ	coil helix angle, ^{o}
μ	fluid dynamic viscosity, kg/ms
α	corrugation helix angle, ^{o}
β	coefficient of isobaric thermal expansion, K^{-1}
ρ	density of the fluid, kg/m^3
L_T	length of twisted-tape, m
L	axial length, length of the duct, m
$\dot{m}$	mass flow rate, kg/s
Nu_m	axially averaged Nusselt number, dimensionless
ΔP_z	pressure drop, mm
$\Delta P^{'}$	pressure drop, N/m^2
P	rib pitch, m
Pr	fluid Prandtl number, dimensionless
Ra	Rayleigh number, dimensionless
Re_{ax}	Reynolds number based on axial velocity, dimensionless
Re_{sw}	Reynolds number based on swirl velocity, dimensionless
Re	Reynolds number based on plain duct diameter, dimensionless
Sw	swirl parameter, dimensionless
T	temperature, K

t	tape thickness, m
ΔT_w	wall to fluid bulk temperature difference, K
V_a	mean axial velocity, m/s
V_o	mean velocity based on plain duct diameter, m/s
V_s	actual swirl velocity at duct, m/s
X	Pr^n, the value of n depends on the exponent of Pr in the correlation
y	twist ratio, dimensionless
z	axial length, the distance between the measuring pressure taps, m
Y	$\left(\frac{\mu_b}{\mu_w}\right)^{-0.14} \times \frac{1}{5.172}$, dimensionless

REFERENCES

[1] Meyer, J. P., and Olivier, J. A., 2011, "Transitional flow inside enhanced tubes for fully developed and developing flow with different types of inlet disturbances: Part II–Heat Transfer." International Journal of Heat and Mass Transfer 54(7-8), pp. 1598-1607.DOI: 10.1016/j.ijheatmasstransfer.2010.11.026

[2] Du Plessis, J. P., and Kroger, D. G., 1983,"Numerical prediction of laminar flow with heat transfer in tube with a twisted tape insert." In Proceedings of the International Conference on Numerical Methods in Laminar and Turbulent Flow, pp. 775-785.

[3] Seemawute, P., and Eiamsa-Ard, S., 2010, "Thermohydraulics of turbulent flow through a round tube by a peripherally-cut twisted tape with an alternate axis." International Communications in Heat and Mass Transfer 37(6), pp. 652-659. DOI: 10.1016/j.icheatmasstransfer.2010.03.005

[4] Manglik, R. M., and Bergles, A. E., 1993, "Heat transfer and pressure drop correlations for twisted-tape inserts in isothermal tubes: Part II—Transition and turbulent flows." Journal of Heat Transfer 115 (4), pp. 890-896. DOI: 10.1115/1.2911384

[5] Saha, S. K., 2010,"Thermal and friction characteristics of laminar flow through rectangular and square ducts with transverse ribs and wire coil inserts." Experimental Thermal and Fluid Science 34(1), pp. 63-72. DOI: 10.1016/j.expthermflusci.2009.09.003

[6] Pal, S., and Saha, S. K., 2015,"Laminar fluid flow and heat transfer through a circular tube having spiral ribs and twisted tapes." Experimental Thermal and Fluid Science, 60 pp. 173-181. DOI: 10.1016/j.expthermflusci.2014.09.005

[7] Saha, S. K., Gaitonde, U. N., and Date, A. W., 1989, "Heat transfer and pressure drop characteristics of laminar flow in a circular tube fitted with regularly spaced twisted-tape elements." Experimental Thermal and Fluid Science, 2(3) pp. 310-322. DOI: 10.1016/0894-1777(89)90020-4

[8]Xie, L., R. Gu, and X. Zhang., 1992, "A study of optimum inserts for enhancing convective heat transfer of high viscosity fluid in a tube." Multiphase Flow and Heat Transfer. In Second International Symposium, vol. 1, pp. 649-656.

[9] Thiangpong, C., Eiamsa-Ard, P., Promvonge, P., and Eiamsa-Ard, S., 2012, "Effect of perforated twisted-tapes with parallel wings on heat tansfer enhancement in a heat exchanger tube." Energy Procedia, 14: 1117-1123. DOI: 10.1016/j.egypro.2011.12.1064

[10] Eiamsa-Ard, S., and Promvonge, P., 2010."Thermal characteristics in round tube fitted with serrated twisted tape." Applied Thermal Engineering, 30(13), 1673-1682. DOI: 10.1016/j.applthermaleng.2010.03.026

[11] Eiamsa-Ard, S., and Seemawute, P., 2012, "Decaying swirl flow in round tubes with short-length twisted tapes." International Communications in Heat and Mass Transfer 39(5), pp. 649-656. DOI: 10.1016/j.icheatmasstransfer.2012.03.021

[12] Krishna, S. R., Pathipaka, G., and Sivashanmugam, P., 2009, "Heat transfer and pressure drop studies in a circular tube fitted with straight full twist." Experimental Thermal and Fluid Science 33(3), pp.431-438. DOI:10.1016/j.expthermflusci.2008.10.007

[13] Bhuiya, M. M. K., Sayem, A. S. M., Islam, M., Chowdhury, M. S. U., and Shahabuddin, M., 2014, "Performance assessment in a heat exchanger tube fitted with double counter twisted tape inserts." International Communications in Heat and Mass Transfer 50, pp. 25-33. DOI: 10.1016/j.icheatmasstransfer.2013.11.005

[14] Ray, S., and Date, A. W., 2003, "Friction and heat transfer characteristics of flow through square duct with twisted tape insert." International Journal of Heat and Mass Transfer 46(5) , pp. 889-902. DOI: 10.1016/S0017-9310(02)00355-1

[15] Hong, S. W., and Bergles, A. E., 1976, "Augmentation of laminar flow heat transfer in tubes by means of twisted-tape inserts." Journal of Heat Transfer 98(2), pp. 251-256. DOI:10.1115/1.3450527

[16] Date, A. W., 1974,"Prediction of fully-developed flow in a tube containing a twisted-tape." International Journal of Heat and Mass Transfer 17(8), pp. 845-859. DOI: 10.1016/0017-9310(74)90152-5

[17] Date, A. W., and Gaitonde, U. N., 1990, "Development of correlations for predicting characteristics of laminar flow in a tube fitted with regularly spaced twisted-tape elements." Experimental Thermal and Fluid Science 3(4), pp. 373-382. DOI: 10.1016/0894-1777(90)90035-6

[18] Saha, S. K., and Dutta, A., 2001, "Thermo-hydraulic study of laminar swirl flow through a circular tube fitted with twisted tapes." Journal of Heat Transfer 123(3), pp. 417-427. DOI:10.1115/1.1370500

[19] Han, J. C., 1988, "Heat transfer and friction characteristics in rectangular channels with rib turbulators." Journal of Heat Transfer 110(2), pp. 321-328. DOI:10.1115/1.3250487

[20] Shivkumar, C., and Raja Rao, M., 1988, "Studies on compound augmentation of laminar flow heat transfer to generalized power law fluids in spirally corrugated tubes by means of twisted tape inserts." ASME, HTD, 96 pp. 685-692.

[21]Saha, S. K., B. K. Barman, and S. Banerjee., 2012, "Heat transfer enhancement of laminar flow through a circular tube having wire coil inserts and fitted with center-cleared twisted tape." Journal of Thermal Science and Engineering Applications 4(3), 031003. DOI:10.1115/1.4006289

[22] Saha, S., and S. K. Saha., 2013,"Enhancement of heat transfer of laminar flow of viscous oil through a circular tube having integral helical rib roughness and fitted with helical screw-tapes." Experimental Thermal and Fluid Science 47, pp. 81-89. DOI.org/10.1016/j.expthermflusci.2013.01.003

[23] Saha, S. K., and G. L. Dayanidhi., 2012, "Thermo-fluid characteristics of laminar flow of viscous oil through a circular tube having integral helical corrugations and fitted with centre-cleared twisted-tape." Heat and Mass Transfer 48(12), pp.2059-2068.

[24] Saha, S. K., 2010, "Thermohydraulics of turbulent flow through rectangular and square ducts with axial corrugation roughness and twisted-tapes with and without oblique teeth." Experimental Thermal and Fluid Science 34(6), pp. 744-752. DOI.org/10.1016/j.expthermflusci.2010.01.003

[25] Patil, A. G., 2000, "Laminar flow heat transfer and pressure drop characteristics of power-law fluids inside tubes with varying width twisted tape inserts." Journal of Heat Transfer 122, pp. 143-149. DOI:10.1115/1.521448

[26] Wongcharee, K., and Eiamsa-Ard., S., 2011, "Friction and heat transfer characteristics of laminar swirl flow through the round tubes inserted with alternate clockwise and counter-clockwise twisted-tapes." International Communications in Heat and Mass Transfer 38(3), pp. 348-352. DOI:10.1016/j.icheatmasstransfer.2010.12.007

[27] Eiamsa-Ard, S., Thianpong, C., and Eiamsa-Ard, P., 2010, "Turbulent heat transfer enhancement by counter/co-swirling flow in a tube fitted with twin twisted tapes." Experimental Thermal and Fluid Science 34(1), pp. 53-62. DOI:10.1016/j.expthermflusci.2009.09.002

[28] Webb, R. L., and Kim, N. Y., 2005, "Enhanced heat transfer." Taylor and Francis, NY. ISBN 9781591690146

[29] Sheikholeslami, M, Jafaryar, M., A. Ali, Jagar, Mustafa Samir Hamad, Li Zhixiong, 2019, "Simulation of turbulent flow of nanofluid due to existence of new effective turbulator involving entropy generation", Journal of Molecular Liquids, Volume 291, 1 October 2019, 111283, https://doi.org/10.1016/j.molliq.2019.111283

[30] Sheikholeslami, M, Jafaryar, M.,, Shafee, Ahmad, Li Zhixiong, 2018, "Investigation of second law and hydrothermal behavior of nanofluid through a tube using passive methods", Journal of Molecular Liquids, Volume 269, 407-416

[31]Sheikholeslami, M., Jafaryar, M., Hedayat, Mohammadali, Shafee, Ahmad, Bakouri, Mohsen, 2019, "Heat transfer and turbulent simulation of nanomaterial due to compound turbulator including irreversibility analysis", Int. J. Heat Mass Transfer, 137, 1290-1300

[32]Sheikholeslami M., Jafaryar M., Shafee, Ahmad, Li, Zhixiong, Haq, Rizwan-ul 2019, "Heat transfer of nanoparticles employing innovative turbulator considering entropy generation", Int. J Heat Mass Transfer, 136, 1233-1240

[33] Farshad, Seyyed Ali, Sheikholeslami, M., 2019, Nanofluid flow inside a solar collector utilizing twisted tape considering exergy and entropy analysis, Renewable Energy, 141, 246-258

[34] Kline, S. J., and McClintock, F. A., 1953, "Describing Uncertainties in Single Sample Experiments." Mech. Eng., 75(1), pp. 3–8

[35] Bergles, A. E., Blumenkrantz, A. R., and Taborek, J., 1974, "Performance evaluation criteria for enhanced heat transfer surfaces." In International Heat Transfer Conference Digital Library. Begel House Inc.